

# **REDUCTION IN OSCILLATION OF A SUSPENDED LOAD IN OVERHEAD CRANES**

By

**Tahir Ilyas**

(2006-NUST-MSc PhD-Elec-17)



Submitted to the Department of Electrical Engineering  
In Partial Fulfillment of the requirements for the Degree of

Master of Science  
In  
Electrical Engineering

**Thesis Advisor**

Dr. Ejaz Muhammad

**College of Electrical and Mechanical Engineering  
National University of Sciences and Technology, Pakistan**

**2008**



In the name of Allah, the most Merciful and the most  
Beneficent

# **ABSTRACT**

## **REDUCTION IN OSCILLATION OF A SUSPENDED LOAD IN OVERHEAD CRANES**

By

**Tahir Ilyas**

Movement of heavy loads using overhead cranes is a very important process in industry. Moving a suspended load causes undesirable swings which develop oscillations. It is desirable to reduce amplitude of Oscillation at the beginning and termination of desired movement.

The objective of this research was to utilize the experts knowledge and design a system for efficient control of crane with minimum load oscillations. Two approaches have been used to control the crane

1. Open Loop Drive signal Shaping
2. Closed loop Drive signal Shaping

Open loop method is limited to ensuring that the load will not be oscillating or have minimal swing after a transition from its rest position to another constant speed( provided that the load was initially not swinging). In this technique, it has been kept in mind that the acceleration / deceleration must remains gradual to prevent jerking to suspended load. The hardware has also been implemented for this technique.

In closed loop method, Fuzzy logic has been used to utilize hoist angle for generating feedback to control movement of trolley. Hardware implementation has not been done, however its working efficiency has been demonstrated through simulation.

*TO MY WIFE, PARENTS AND TEACHERS*

# Acknowledgments

First I would like to thank Allah almighty for his guidance and my parents for their endless prayers. I also express my immense regards to my wife for her endless patience, support and encouragement to complete my research.

It was great owner for me to work under the able guidance of **Dr. Ejaz Muhammad** whose charismatic personality remained a source of motivation for me to complete my research work in stipulated time. His valuable guidance enabled me to move in right direction without wasting time. I am indebted to **Dr Khalid Munawar** and **Dr Mohammad Bilal Malik**, who permitted me to avail the facilities of Control Lab for my research work. I would like to especially thank **Dr. Khalid Munawar** for his keen interest in my project and for his valuable guidance through out my work.

I would also like to extend my thanks to all of my friends of the Nonlinear Control Lab who bore with my non ending questions and replied all of them, especially **Mr. Asim Ejaz** and **Mr. Muhammad Usman** who helped me a lot in solving my Matlab simulation problems through their tremendous knowledge. In addition, I would like to thank **Major Salman** for his guidance in solving hardware related problems. In addition to their unlimited help in these past six months, they were the best friends and company I found.

# Table of Contents

<b>1.</b>	<b>Introduction to Cranes</b>	
1.1	Introduction .....	1
1.2	Types of Cranes in the Industry .....	1
1.3	Literature Review .....	4
1.4	Objective .....	5
<b>2.</b>	<b>Mathematical Modeling</b>	
2.1	Model Description .....	6
2.2	System Parameters .....	7
2.3	Derivation of the Equations of Motion .....	9
2.4	State-Space Model of the Crane .....	13
<b>3.</b>	<b>Open Loop Oscillation Reduction</b>	
3.1	Introduction .....	15
3.2	Properties of Pendulum .....	16
3.3	Oscillation Damping	
3.3.1	For Longer run .....	17
3.3.2	For Inching operation .....	23
3.4	Limitations of the Method .....	25
<b>4.</b>	<b>Fuzzy Logic Controlled Crane</b>	
4.1	Introduction to Fuzzy Logic .....	26
4.2	Fuzzy Logic Controller Design .....	27
4.2.1	Radial Controller .....	29
4.2.1a	Tracking FIE .....	29
4.2.1b	Oscillation Damping FIE .....	32
4.2.2	Rotational Controller.....	34

4.2.2a	Tracking FIE .....	34
4.2.2b	Oscillation Damping FIE .....	37
4.3	Simulation Results .....	40
4.3.1	Radial Case .....	40
4.3.2	Rotational Case .....	42
4.3.3	Compound Case .....	46
4.3.4	Damping Case .....	47
<b>5.</b>	<b>Conclusions and Recommendations</b>	
5.1	Conclusion .....	52
5.2	Recommendations .....	53
<b>Annexure</b>	.....	<b>55</b>
<b>Bibliography</b>	.....	<b>59</b>
 <b>List of Figures</b>		
1.1	Gantry crane .....	2
1.2	Rotary crane .....	3
1.3	Boom cranes .....	3
2.1	3-D model of a rotary crane .....	6
2.2	Side view of the crane showing the in-plane angle $\phi$ ....	8
2.3	Oscillation angles $\Phi(t)$ and $\theta(t)$ of the load .....	9
3.1	Graphical representation of Crane .....	18
3.2	Acceleration profile .....	20
3.3	Interconnection block diagram .....	21
3.4	Lab model of Crane .....	22

3.5	Control Circuit for generation of DC drive input to produce required acceleration .....	22
4.1	Example on fuzzy logic sets .....	27
4.2	System block diagram with fuzzy logic controller .....	27
4.3	Fuzzy logic controller design .....	28
4.4	Two FIEs are inside each FLC .....	28
4.5	Fuzzification of $E_r(t)$ .....	30
4.6	Fuzzification of $E_r^{\&}(t)$ .....	30
4.7	Fuzzy sets of $\&_{Track}(t)$ .....	31
4.8	Fuzzification of $f(t)$ .....	32
4.9	Fuzzification of $f^{\&}(t)$ .....	33
4.10	Defuzzification of $\&_{Correction}$ .....	33
4.11	Fuzzification of $E_g(t)$ .....	35
4.12	Fuzzification of $E_g^{\&}(t)$ .....	35
4.13	Defuzzification of $\&_{Track}$ .....	36
4.14	Fuzzification of $q(t)$ .....	37
4.15	Fuzzification of $q^{\&}(t)$ .....	38
4.16	Defuzzification of $\&_{Correction}$ .....	39
4.17	Operator radial signal .....	40
4.18	Uncontrolled Vs Controlled In-plane angle $f(t)$ for the radial using the fuzzy controller .....	41
4.19	Desired and actual distance for the Radial case Using the fuzzy controller .....	42



4.20	Operator rotational signal .....	43
4.21	Uncontrolled Vs Controlled In-plane angle $f(t)$ for the rotational case using the fuzzy controller .....	43
4.22	Uncontrolled Vs Controlled Out-of-plane angle $q(t)$ for the rotational case using the fuzzy controller .....	44
4.23	Desired and actual Radial distance for the rotational case using the fuzzy controller .....	45
4.24	Desired and actual Rotational angle for the rotational case using the fuzzy controller .....	45
4.25	Uncontrolled Vs Controlled In-plane angle $f(t)$ for the compound case using the fuzzy controller .....	46
4.26	Uncontrolled Vs Controlled Out-of-plane angle $q(t)$ for the compound case using the fuzzy controller .....	47
4.27	Desired and actual Radial distance for the compound case using the fuzzy controller .....	48
4.28	Desired and actual Rotational angle for the compound case using the fuzzy controller .....	48
4.29	Uncontrolled Vs Controlled In-plane angle $f(t)$ for the damping case using the fuzzy controller .....	49
4.30	Uncontrolled Vs Controlled Out-of-plane angle $q(t)$ for the damping case using the fuzzy controller .....	50
4.31	Desired and actual Radial distance for the damping case using the fuzzy controller .....	50
4.32	Desired and actual Rotational angle for the damping case using the fuzzy controller .....	51

## List of Tables

4.1	Rules for the radial tracking FIE .....	31
4.2	Rules for the radial oscillations damping FIE .....	34
4.3	Rules for the rotational tracking FIE .....	36
4.4	Rules for the rotational oscillations damping FIE .....	38

# **CHAPTER-1**

## **INTRODUCTION TO CRANES**

### **1.1 Introduction**

A crane is considered as one of the most important machine used in industry to transfer loads and cargo from one location to another. Overhead cranes are used to support and transport loads suspended by a variable length rope hoist. The hoist is attached to a carriage which is traversed along a track. It is desirable to reduce oscillations of the load when it is moved by the crane. Operators controlling the cranes drive them very slowly and cleverly to avoid undue oscillations, which in turn leads to wasting time and reduced efficiency. Since most of the cranes are operated manually, so their performance is operator dependent. With the size of these cranes becoming larger, controlling becomes even more tricky and a higher level of expertise on the part of operator become more essential.

In modern cranes, the methods of damping load oscillations have focused on generating a drive signal that, when applied to the input of the motor controls the travel of the carriage and reduces load swinging. Mainly two control methods have been used to suppress load oscillations. Open loop methods shape the drive signal considering the properties of pendulum. Most of the closed loop damping methods uses angular deviation of the hoisting rope from its rest position as feedback to shape the drive signal. In such closed loop methods, the shape and magnitude of drive signal corresponds to the magnitude of the deviation of the rope.

### **1.2 Types of Cranes in the Industry**

Cranes can be classified in terms of their mechanical structures and dynamics into three types: gantry, rotary, and boom cranes.

**Gantry cranes (Figure 1.1)** are characterized by a trolley moving over a jib (girder), the trolley motion can be carried out in two dimensions by mounting the jib on another set of orthogonal railings, called bridge cranes. In this case, the trolley can move in a two-dimensional horizontal plane. They are common in factories because of their low cost, ease of assembly, and maintenance. They are also used in mines, steel-mill productions lines, and transport industry.



**Figure 1.1:** Gantry crane <sup>[1]</sup>.

**A rotary crane (Figure 1.2)** consists of a jib that rotates in a horizontal plane around a fixed vertical axis. The trolley that holds the load can move radially over the jib. Hence, the combined motion of the trolley and jib can place the load at any point in the horizontal plane within the reach of the crane.

**Boom cranes (Figure 1.3)** are very common on ships and in harbors. In general, a boom crane consists of a rotating base to which a boom is attached. The load hangs from the tip of the boom by a set of cables and pulleys. The rotational movement of the base along with the luff movement of the boom places the boom tip over any point in the horizontal plane, that is in reach of the crane. Meanwhile, changing the elevation (luff) angle of the boom causes a



**Figure 1.2:** Rotary crane <sup>[2]</sup>.



**Figure 1.3:** Boom cranes.

Change in the radial and vertical positions of the load. The structure of boom cranes supports loads in compression, whereas rotary and gantry cranes support loads in a bending fashion. This makes boom cranes more compact than rotary and gantry cranes of similar capacities. Boom cranes are mounted on ships to transfer cargo between ships or on harbor pavements to transfer cargo between ships and offshore structures.

## Literature Review

Several researchers have investigated the control of rotary cranes and considered different input shaping techniques to bring the load to rest at the end point of a predefined motion profile. Myung Soo Moon<sup>[3]</sup>, Nalley and Trabia<sup>[4]</sup> applied fuzzy logic controller to a bi-directional gantry crane. They introduced the idea of using two separate fuzzy controllers each of which has two fuzzy inference engines: one to track the desired position commanded by the operator and another to correct for payload oscillations. After performing all of the required calculations, the outputs of the two engines are combined to obtain the final control signal. The controller was used to drive the crane along a path generated by an input-shaping strategy. They obtained good results for damping the oscillations and at the same time reducing the payload travel time. Z. N. Masoud, A. H. Nayfeh<sup>[5]</sup> developed a time-delayed position feedback controller. The controller targeted boom cranes with base excitations. The controller forces the suspension point of the payload to follow an operator commanded motion to which a correction is added. The correction consists of a time-delayed percentage of the payload motion relative to the suspension point.

Good results were obtained for damping the oscillations and at the same time reducing the payload travel time. Although the following discussion is directed at other types of cranes, it is useful and relevant to our design of controllers.

## **1.3 Objective**

The objective of this work is to find a control strategy to transfer loads using overhead cranes. The control strategy should take into account two main factors. First, the time needed to move the payload from the initial pick up point to the destination point must be minimized. Second, the oscillation of the payload must be reduced to prevent hazards of damage to the surrounding equipment and to load itself.

# Chapter 2

## Mathematical Modeling

In this chapter, we give a complete description of the crane model, a derivation of the equations of motion, and the corresponding state-space model. To derive a set of equations of motion that model the system dynamics, we have used the Lagrangian approach.

### 2.1 Model Description

A rotary crane consists of a trolley that moves radially along a rotating jib. The jib rotates in a horizontal plane. The combined movements of the jib and the trolley enable positioning of the trolley and consequently the load over any point in the work space. The variation in the length of the hoisting cable is important for picking up the load, putting it down, and moving it away from obstacles. It also can be used as a part of the control strategy.

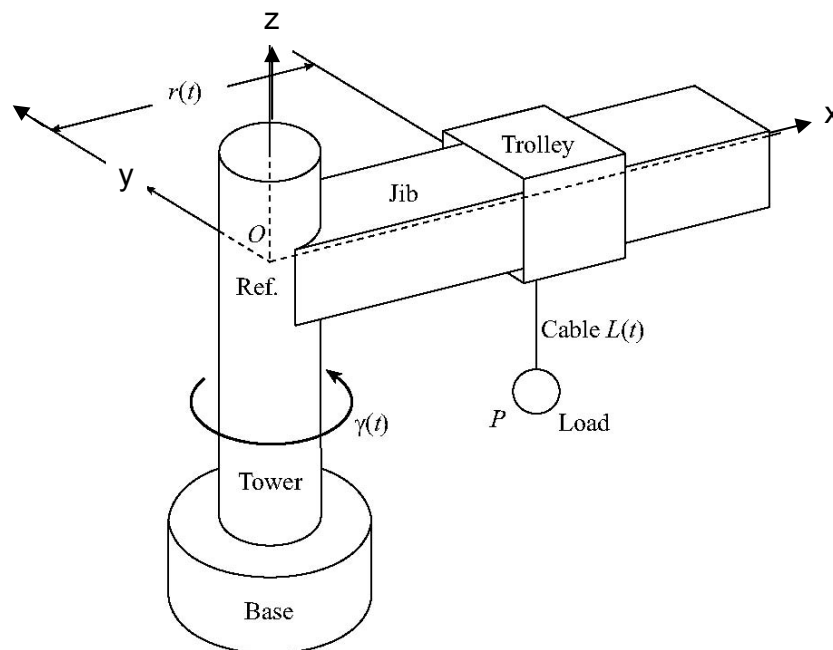


Figure 2.1: A 3D model of a rotary crane<sup>[5]</sup>.



As shown in Figure 2.1, the structure of the crane consists of

- (a) A tower that holds the jib of the crane; it is responsible for the rotational motion of the crane.
- (b) A base that is usually fixed to the ground to prevent any oscillations.
- (c) A jib that is mounted to the tower.
- (d) A trolley that slides over the jib in a transverse direction.
- (e) A suspension system of cables and pulleys. In the very general case, the length of the cable can be changed during load transport or at least at the pickup and end points. *The process of changing the cable length is called hoisting.*

## 2.2 System Parameters

To derive the equations of motion, one needs to define clearly the system parameters. As shown in Figure 2.1, a right-handed Cartesian coordinate system (xyz) is centered at a reference point that lies in the plane of the jib at the center of the crane tower, with its positive z-axis being along the tower upward axis. The x and y -axes are in the plane of the jib, with the x-axis being along the jib. The xyz coordinate system is attached to the moving jib. The jib rotates and traces an angle  $g(t)$ . The trolley moves on the jib with its position  $r(t)$  being the distance measured from the reference point of the xyz coordinate system to the suspension point of the payload cable on the trolley. The angle  $g(t)$  and the radial distance  $r(t)$  are the inputs to the system. They are used to control the system behavior. We model the load as a point mass. The interaction between the load dynamics and the crane dynamics is neglected due to the assumption that the mass of the crane being very large compared to that of the load. We start by defining the velocity of the trolley in the jib-fixed coordinate system as

$$v_x = \dot{r} \quad \dots\dots (2.1)$$

and its acceleration is

$$a_x = \ddot{x} \quad \dots\dots (2.2)$$

The angular velocity of the jib is

$$\omega = \dot{\theta} \quad \dots\dots (2.3)$$

and its angular acceleration is

$$a = \ddot{\theta} \quad \dots\dots (2.4)$$

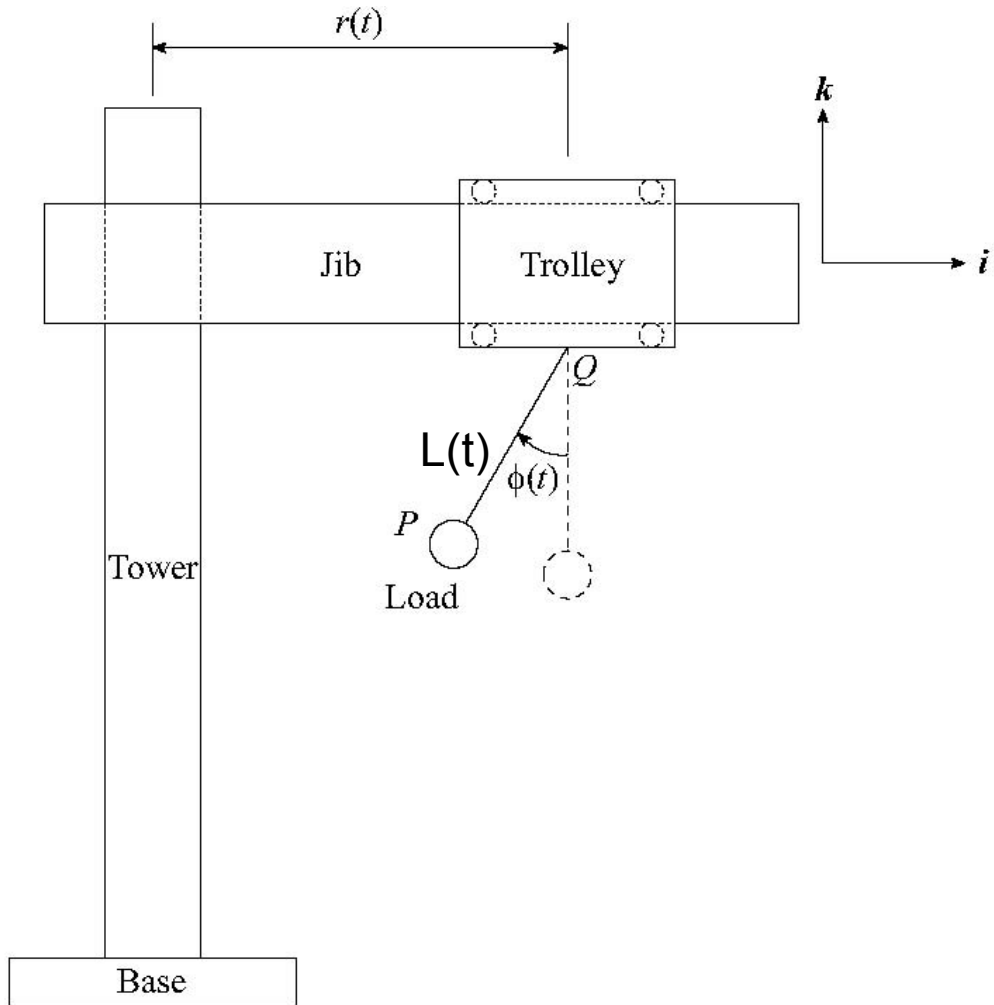


**Figure 2.2:** Side view of the crane showing the in-plane angle  $\phi(t)$  [5].

The load pendulations are characterized by two angles,  $f(t)$  and  $q(t)$ . The angle  $f(t)$  is the angle which the cable makes with the z-axis in the xz-plane, as shown in Figure 2.2. The out-of-plane angle  $q(t)$  is the angle which the cable makes with the xz-plane. So it is clear now that the objective of the controller is to move the payload while keeping  $f(t)$  and  $q(t)$  as small as possible.

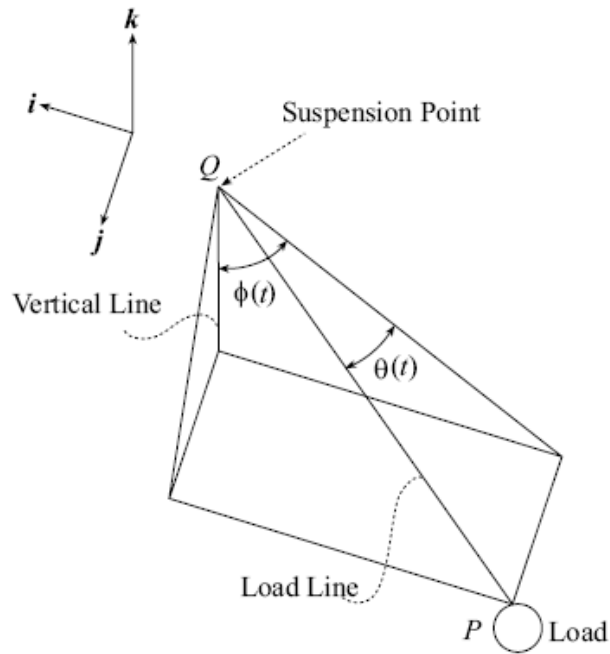


**Figure 2.3:** Oscillation angles  $f(t)$  and  $q(t)$  of the load.

## 2.3 Derivation of the Equations of Motion <sup>[5,6,7,8]</sup>

The first step in deriving the equations of motion using the Lagrangian approach is to find the position  $P(t)$  of the load with respect to the reference point  $O$ . In the jib-fixed coordinate system, the load position is

$$P(t) = [r(t) - L(t) \cos \theta(t)]i + [L(t) \sin \theta(t)]j$$

$$+[L(t)\cos\theta(t)\cos\phi(t)]k \quad \dots\dots (2.5)$$

To determine the kinetic energy of the load, we need to determine the velocity  $\dot{p}(t)$  of the load. Since the jib is moving

$$\dot{p}(t) = \frac{\partial p(t)}{\partial t} + \omega(t) \times p(t) \quad \dots\dots (2.6)$$

Where

$$\omega(t) = \dot{\gamma}(t)k \quad \dots\dots (2.7)$$

Hence, the absolute velocity of the payload is

$$\begin{aligned} \dot{p}(t) = & [\dot{\gamma}(t) - \dot{L}(t)\sin\phi(t)\cos\theta(t) - L(t)\{\dot{\gamma}(t)\sin\theta(t) \\ & - \dot{\theta}(t)\sin\theta(t)\sin\phi(t) + \dot{\phi}(t)\cos\theta(t)\cos\phi(t)\}]i \\ & + [\dot{L}(t)\sin\theta(t) + r(t)\dot{\gamma}(t) + L(t)\cos\theta(t)\{\dot{\theta}(t) - \dot{\gamma}\sin\phi(t)\}]j \\ & + [-\dot{L}(t)\cos\theta(t)\cos\phi(t) + L(t)\{\dot{\theta}(t)\sin\theta(t)\cos\phi(t) \\ & + \dot{\phi}(t)\sin\phi(t)\cos\theta(t)\}]k \quad \dots\dots (2.8) \end{aligned}$$

The kinetic energy of the load is

$$K_E = \frac{1}{2}m_{Load}[\dot{P}(t).\dot{P}(t)] \quad \dots\dots (2.9)$$

Or

$$\begin{aligned} K_E = & \frac{1}{2}m_{Load}[\{\dot{L}(t)\sin\theta(t) + r(t)\dot{\gamma}(t) + L(t)\cos\theta(t)(\dot{\theta}(t) \\ & - \dot{\gamma}(t)\sin\theta(t))\}^2 + \{\dot{r}(t) - \dot{L}(t)\sin\phi(t)\cos\theta(t) - \\ & L(t)(\dot{\gamma}(t)\sin\theta(t) - \dot{\theta}(t)\sin\theta(t)\sin\phi(t) + \dot{\phi}(t)\cos\theta(t) \\ & \cos\phi(t))\}^2 + \{-\dot{L}(t)\cos\phi(t)\cos\theta(t) + L(t)(\dot{\theta}(t)\sin\theta(t) \\ & \cos\phi(t) + \dot{\phi}(t)\cos\theta(t)\sin\phi(t))\}^2] \quad \dots\dots (2.10) \end{aligned}$$

The potential energy of the payload is given by

$$P_E = -m_{Load}gL(t)\cos\theta(t)\cos\phi(t) \quad \dots\dots (2.11)$$

Finally the Lagrangian  $L$  is given by

$$L = K_E + P_E \quad \dots\dots$$

(2.12)

$$\begin{aligned} L = & \frac{1}{2}m_{Load}[\{2gL(t)\cos\theta(t)\cos\phi(t) + \dot{L}(t)\sin\theta(t) + r(t)\dot{\gamma}(t) \\ & + L(t)\cos\theta(t)(\dot{\theta}(t) - \dot{\gamma}(t)\sin\theta(t))\}^2 + \{\dot{r}(t) - \dot{L}(t)\sin\phi(t)\cos\theta(t) \\ & - L(t)(\dot{\gamma}(t)\sin\theta(t) - \dot{\theta}(t)\sin\theta(t)\sin\phi(t) + \dot{\phi}(t)\cos\theta(t)\cos\phi(t))\}^2 \\ & + \{-\dot{L}(t)\cos\phi(t)\cos\theta(t) + L(t)(\dot{\theta}(t)\sin\theta(t)\cos\phi(t) \\ & + \dot{\phi}(t)\cos\theta(t)\sin\phi(t))\}^2] \quad \dots\dots (2.13) \end{aligned}$$

Euler Lagrangian equation<sup>[6]</sup> corresponding to  $L$  is

$$\frac{d}{dt}\left(\frac{\partial L}{\partial \dot{x}_i}\right) - \left(\frac{\partial L}{\partial x_i}\right) = 0 \quad \dots\dots (2.14)$$

where  $x_1 = q$  and  $x_2 = f$ . This will yield the following two nonlinear equations of motion:

$$\begin{aligned} L(t)\ddot{\theta}(t) + 2\dot{L}(t)\dot{\theta}(t) - 2L(t)\dot{\gamma}(t)\cos\phi(t)\cos^2\theta(t)\dot{\phi}(t) + \frac{1}{2}L(t)\sin 2\theta(t)\dot{\phi}^2(t) \\ - \frac{1}{2}L(t)\dot{\gamma}^2(t)\sin 2\theta(t)\cos^2\phi(t) + g\sin\theta(t)\cos\phi(t) + 2\dot{r}(t)\dot{\gamma}(t)\cos\theta(t) \\ - r(t)\dot{\gamma}^2(t)\sin\phi(t)\sin\theta(t) + \ddot{r}(t)\sin\theta(t)\sin\phi(t) - 2\dot{L}(t)\dot{\gamma}(t)\sin\phi(t) \\ + r(t)\ddot{\gamma}(t)\cos\theta(t) - L(t)\ddot{\gamma}(t)\sin\phi(t) = 0 \quad \dots\dots (2.15) \end{aligned}$$

and

$$\begin{aligned}
 & L(t) \cos \theta(t) \ddot{\phi}(t) + 2\dot{L}(t) \cos \theta(t) \dot{\phi}(t) + 2L(t) \dot{\gamma}(t) \cos \theta(t) \cos \phi(t) \dot{\theta}(t) \\
 & - 2L(t) \sin \theta(t) \dot{\theta}(t) \dot{\phi}(t) + g \sin \phi(t) + 2\dot{L}(t) \dot{\gamma}(t) \cos \phi(t) \sin \theta(t) \\
 & + \cos \phi(t) \dot{\gamma}^2(t) [r(t) - L(t) \sin \phi(t) \cos \theta(t)] + L(t) \ddot{\gamma}(t) \cos \phi(t) \sin \theta(t) \\
 & - \ddot{r}(t) \cos \phi(t) = 0 \quad \text{..... (2.16)}
 \end{aligned}$$

For our case, the cable length  $L(t)$  is set equal to a constant value, then

$$\frac{dL}{dt} = 0 \quad \text{..... (2.17)}$$

Substituting equation (2.17) into equations (2.15) and (2.16) yields

$$\begin{aligned}
 & \ddot{\phi}(t) - 2\dot{\gamma}(t) \cos \phi(t) \cos^2 \theta(t) \dot{\phi}(t) + \frac{1}{2} \sin 2\theta(t) \dot{\phi}^2(t) - \frac{1}{2} \dot{\gamma}^2(t) \cdot \\
 & \sin 2\theta(t) \cos^2 \phi(t) + \frac{g}{L} \sin \theta(t) \cos \phi(t) + \frac{2}{L} \dot{r}(t) \dot{\gamma}(t) \cos \theta(t) \\
 & - \frac{1}{L} r(t) \dot{\gamma}^2(t) \sin \phi(t) \sin \theta(t) + \frac{1}{L} \ddot{r}(t) \sin \phi(t) \sin \theta(t) + \frac{1}{L} r(t) \ddot{\gamma}(t) \cdot \\
 & \cos \theta(t) - \ddot{\gamma}(t) \sin \phi(t) = 0 \quad \text{..... (2.18)}
 \end{aligned}$$

And

$$\begin{aligned}
 & \cos q(t) \ddot{f}(t) + 2\dot{g}(t) \cos q(t) \cos f(t) \dot{q}(t) - 2 \sin q(t) \dot{q}(t) \dot{f}(t) \\
 & + \frac{g}{L} \sin f(t) + \cos f(t) \dot{g}^2(t) \left[ \frac{r(t)}{L} - \sin f(t) \cos q(t) \right] \\
 & + \dot{g}(t) \sin q(t) \cos f(t) - \frac{1}{L} \ddot{r}(t) \cos f(t) = 0 \quad \text{..... (2.19)}
 \end{aligned}$$

## 2.4 State-Space Model of the Crane<sup>[3,7]</sup>

For easier manipulation of the crane parameters, we reformulate the equations of motion in state-space form. The following equations are used later to develop the crane dynamic model using SIMULINK<sup>[9]</sup> to simulate the system dynamics. To this end, we let

$$x_1 = q(t) \quad \dots (2.20)$$

$$x_2 = \dot{q}(t) \quad \dots (2.21)$$

$$x_3 = r(t) \quad \dots (2.22)$$

$$x_4 = \dot{r}(t) \quad \dots (2.23)$$

$$x_5 = \ddot{q}(t) \quad \dots (2.24)$$

$$x_6 = \ddot{\dot{q}}(t) \quad \dots (2.25)$$

$$x_7 = \ddot{\dot{r}}(t) \quad \dots (2.26)$$

$$x_8 = \ddot{\dot{g}}(t) \quad \dots (2.27)$$

$$U_1 = \ddot{\dot{u}}(t) \quad \dots (2.28)$$

$$U_2 = \ddot{\dot{g}}(t) \quad \dots (2.29)$$

Hence

$$\ddot{q} = x_5 \quad \dots (2.30)$$

$$\ddot{\dot{q}} = x_6 \quad \dots (2.31)$$

$$\ddot{\dot{r}} = x_7 \quad \dots (2.32)$$

$$\ddot{\dot{g}} = x_8 \quad \dots (2.33)$$

$$\ddot{x}_7 = U_1 = \ddot{x}(t) \quad \dots (2.34)$$

$$\ddot{x}_8 = U_2 = \ddot{x}(t) \quad \dots (2.35)$$

Then, it follows from equations (2.18) and (2.19) that

$$\begin{aligned} \ddot{x}_5 = & -\frac{1}{L}(2g \cos x_2 \sin x_1 + 4x_7 x_8 \cos x_1 - \\ & Lx_8^2 \sin 2x_1 \cos^2 x_2 - 2x_3 x_8^2 \sin x_1 \sin x_2 - \\ & 4Lx_6 x_8 \cos x_2 \cos^2 x_1 + Lx_6^2 \sin 2x_1 + 2\sin x_1 \sin x_2 U_1 \\ & + 2x_3 \cos x_1 U_2 - 2L \sin x_2 U_2) \quad \dots (2.36) \end{aligned}$$

$$\begin{aligned} \ddot{x}_6 = & -\frac{1}{L \cos x_1}(g \sin x_2 + x_3 x_8^2 \cos x_2 - Lx_8^2 \sin x_2 \dots \\ & \cos x_1 \cos x_2 + 2Lx_5 x_8 \cos x_1 \cos x_2 - 2Lx_5 x_6 \sin x_1 \\ & - \cos x_2 U_1 + L \sin x_1 \cos x_2 U_2) \quad \dots (2.37) \end{aligned}$$



# CHAPTER 3

## Open Loop Oscillation Reduction

### 3.1 Introduction

In this portion we have developed an open loop method to dampen load oscillations while inching or moving the crane. In such conventional systems, oscillation damping can be achieved by shaping the drive signal by considering the properties of pendulum. In the succeeding pages, methods of damping load oscillations have focused on generating a drive signal that when applied to the input of the motor drive controlling the horizontal travel of the carriage of the crane, will reduce load swing. Practically, a crane operator moves the crane and the suspended load smartly to prevent swing in the suspended load and allow time for oscillations to dampen. But controlling of the crane in this way entirely depends upon the expertise of the operator and job becomes more of operator dependent than crane itself. This portion summarizes a control algorithm to dampen the oscillations by shaping the drive signal.

### 3.2 Properties of pendulum <sup>[10,11,12]</sup>

A pendulum is an object at the end of a massless string that is attached to a pivot about which it can swing freely. This mass is subjected to a restoring motion that will always accelerate it toward an equilibrium position. When a pendulum is displaced from its place of rest, the restoring force will cause it to swing back and forth about equilibrium position. If the pendulum swings through a small angle (in the range where the function  $\sin(\theta)$  can be approximated as  $\theta$ ), the motion may be approximated as simple harmonic motion. The period of a simple pendulum is significantly affected only by its length and the acceleration of gravity. A pendulum has some interesting properties, concerning its frequency of oscillation:-

- a. The frequency of the pendulum is inversely proportional to the length of the string with which it is suspended i.e. shorter the wire, greater is the frequency.
- b. The frequency is independent of the amplitude of the swing, provided the initial angle is not large. At larger angles, there is a slight change in the frequency.
- c. The frequency is independent of the mass of the bob. In other words a pendulum with a heavy bob will move at the same rate as one with a lighter weight bob. Just like the acceleration of gravity on a falling object is independent of the mass of the object.
- d. Volume of the suspended load (not the weight) does have an effect on the frequency of oscillation. Two identical masses but different volume will generate oscillations at different frequency.

As we know that angular velocity of the pendulum can be derived for any point in its arc by observing that the total energy of total energy of the system is conserved. Thus the sum of the potential energy of bob at some height above the equilibrium position, plus the kinetic energy of the moving bob at that point, is equal to the total energy. However, the total energy is also equal to maximum potential energy when the bob is stationary at its peak height (at angle  $\theta_{\max}$ ). By this means it is possible to compute the velocity of the bob at each point along its arc, which in turn can be used to derive an exact period. The resulting period is given by an infinite series.

$$T = 2\pi \sqrt{\frac{L}{g}} \left( 1 + \frac{1}{4} \sin^2 \frac{\theta_{\max}}{2} + \frac{9}{64} \sin^4 \frac{\theta_{\max}}{2} + \dots \right)$$

Note that for small values of  $\theta_{\max}$ , the value of the sine terms become negligible and the period can be approximated by as

$$T \approx 2\pi \sqrt{\frac{L}{g}}$$

where 'L' is the length of the pendulum measured from the pivot point to the bob's centre of gravity and 'g' is the gravitational acceleration. The simple pendulum assumes that the rod is mass less and that the bob is small, so has negligible angular momentum in itself. A physical pendulum has significant size and mass, and hence a significant moment of inertia. A physical pendulum behaves like a simple pendulum but the expression for the period is little modified as

$$T \approx 2\pi \sqrt{\frac{I}{mgL}}$$

where:

$I$  is the moment of inertia of the pendulum about the pivot point ( $I = mr^2$ ).

$r$  or  $L$  is the distance from the centre of mass to the pivot point.

$m$  is the mass of the pendulum.

### 3.3 Oscillation Damping<sup>[11,12]</sup>

#### 3.3.1 For Longer Run

Technique relates to a method for shaping the drive signal controlling the horizontal motion of a crane to dampen load oscillations when moving the crane at longer distance. A general one direction motion of crane trolley can be shown as Figure 3.1.

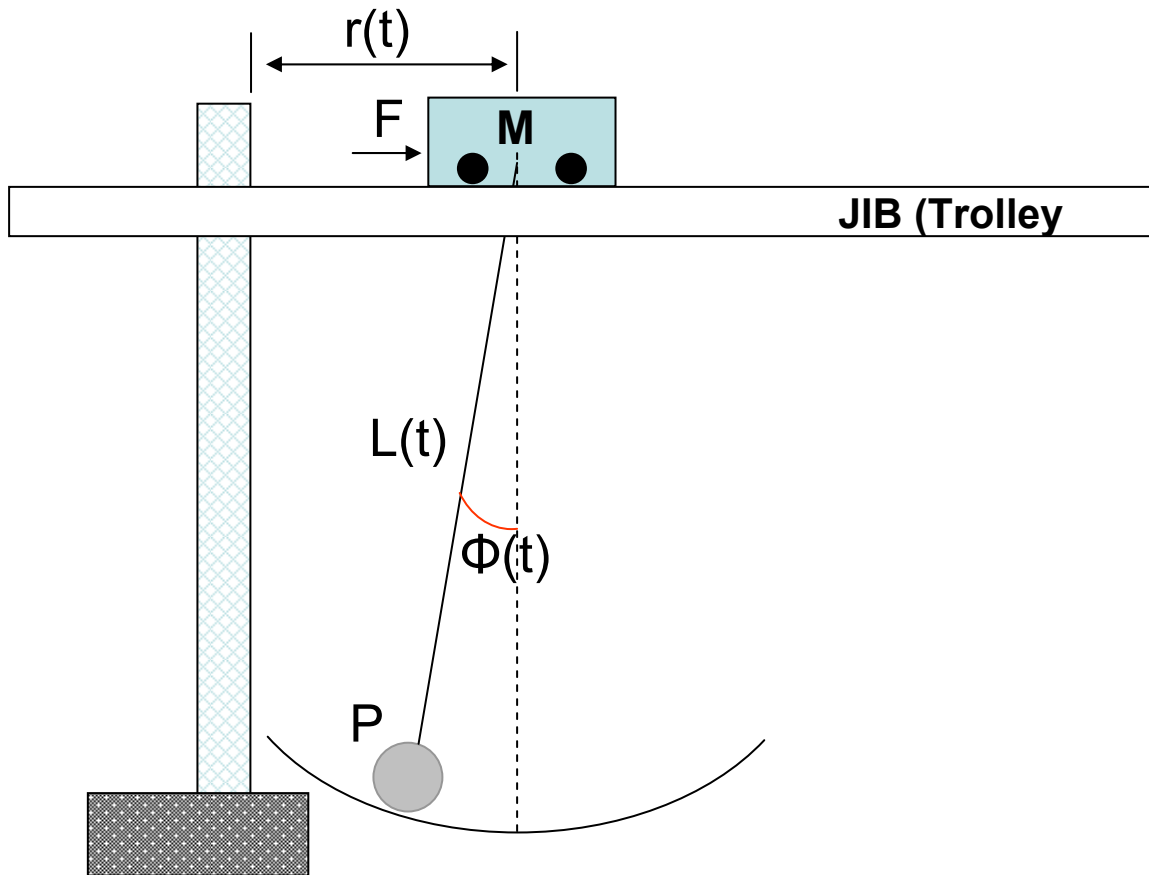


**Figure 3.1:-** Graphical representation of crane<sup>[3]</sup>.

The Oscillation Damping method using open loop drive signal shaping technique is based on following assumptions;-

- a. It is assumed that the load will not be oscillating or have minimal swing at the beginning of a carriage run.
- b. Presumes that no other forces, except gravity and the carriage motor force are acting on the load.

To implement the method, a laboratory model of crane has been made using 12 volt DC motor. Keeping in view the dimensions of the model, input of the carriage motor has been digitized into 16 steps. Each of the step increases the acceleration of the carriage by  $0.02 \text{ m/sec}^2$ . The period of load oscillation is determined by considering the length of hoist and volume of the load. Drive signal has been designed in a manner to control rate of acceleration change in such a

way that when the load is moved first time from its start point / lifting point the motor trolley moves with the smallest acceleration i.e  $0.02 \text{ m/sec}^2$ . The acceleration is maintained for the time equal to  $2T/3$  where  $T$  is the of the period of oscillation of suspended load and then the acceleration is increased to the maximum achievable limit ( which in our case is  $0.32 \text{ m/sec}^2$  in intervals equal to  $T/8(\text{min}) \sim T/6(\text{max})$ . When we give first delay equal to  $2T/3$  and then apply acceleration in incremental steps of  $.02 \text{ m/sec}^2$  . Accelerations applied in this manner dampen the swing during motion and also makes the load to travel at the same velocity as of the trolley. Now, no oscillations will occur while load is in moving state. Basic requirement of this type of load oscillation damping methods is that since changes in speed commands cannot be instantly compensated and certain settling time must elapse before each speed change is compensated and objective of this technique is also to increase the inertia of suspended load in a controlled manner just like the way an expert operator operates it. Operator increases the speed of trolley gradually, takes it to maximum attainable speed and continues traveling.

When the load reaches closer to the destination point, requirement is to reduce the acceleration of trolley in the similar pattern so that the inertia of suspended load is decreased in the same controlled manner. This what an expert does, when the load / trolley reaches near the destination, Operator starts decreasing the speed of trolley to minimum in such a way that by the time load reaches its destination, has minimum speed with no or minimum oscillation. To achieve this we have incorporated a pulse generation arrangement on the operator console. Once the pulse is applied, trolley starts reducing the acceleration at the rate of  $0.02 \text{ m/sec}^2$  in same equal interval of  $T/8 \sim T/6$ . By the time Trolley reaches its destination point the speed will reach to minimum i.e.  $0.02 \text{ m/sec}^2$  and load will have no or minimum Oscillations. Figure 3.2 shows the acceleration profile example of the adopted technique.

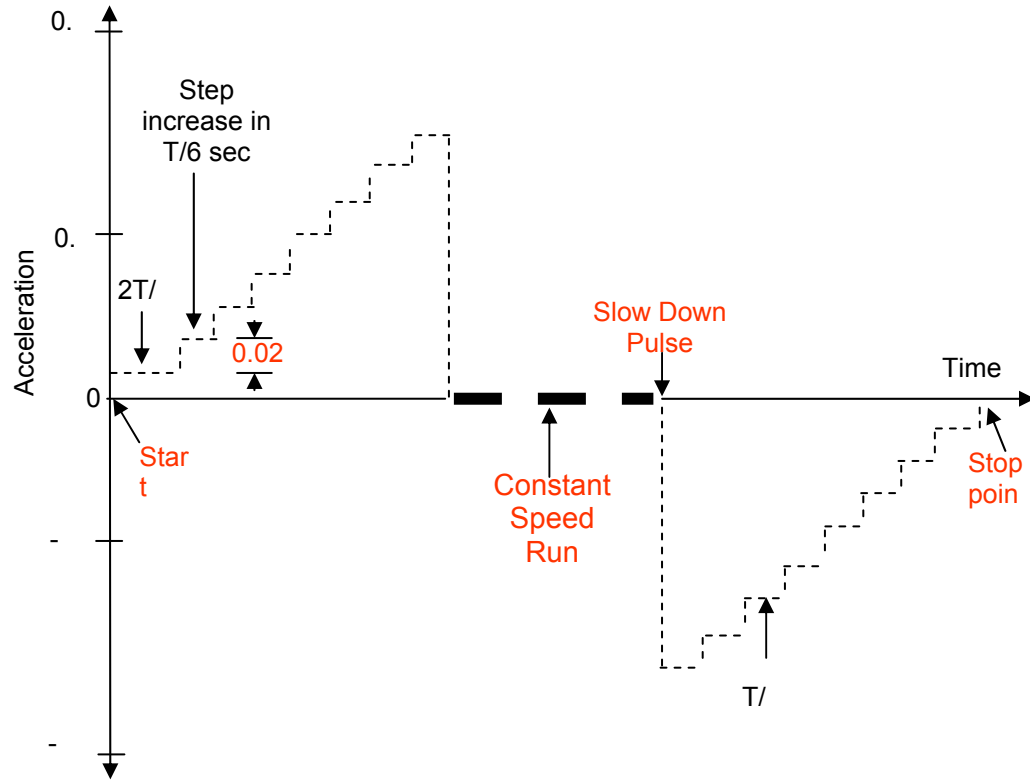


**Figure 3.2:-** Acceleration profile.

Summarizing the above a complete drive signal comprises on three parts which are following:-

- a. The first part of the drive signal which is applied for  $2T/3$  seconds causes carriage displacement very slowly and causes an oscillation of very low amplitude (called Kicking).
- b. The second part of the drive signal is applied after a delay of  $2T/3$  sec from the first signal and consist of step signals separated at  $T/6$  sec (max) to  $T/8$  sec (min) intervals apart . This step changes the velocity of the suspended load gradually. Every time the drive signal is increased a Kick is provided to the suspended load and thereby increasing the velocity of load gradually without any increase in the amplitude of oscillation and so taking the crane to its highest obtainable speed. Now there is no relative velocity between the load and trolley.

- c. Third part of the signal is applied sufficiently in advance of destination point allowing trolley to decelerate in the same fashion without causing oscillations in the suspended load.

To implement the described concept of oscillation reduction, hardware implementation has been done by developing one directional crane model. Block diagram of the system is shown in figure 3.3. A program has been written [13] (refer to Anx-A) for calculation of T corresponding to hoist length and weight of the suspended Load. Software generates a signals for the control circuit which in response generates the required signal for the drive motor. Lab setup and hardware of control circuit is shown in figure 3.4 and 3.5. Hoist length is continuously monitored by using input from the Optical encoder attached with the hoisting mechanism. Software continue recalculating the period of oscillation and readjust the drive signal according to change in the hoist length.

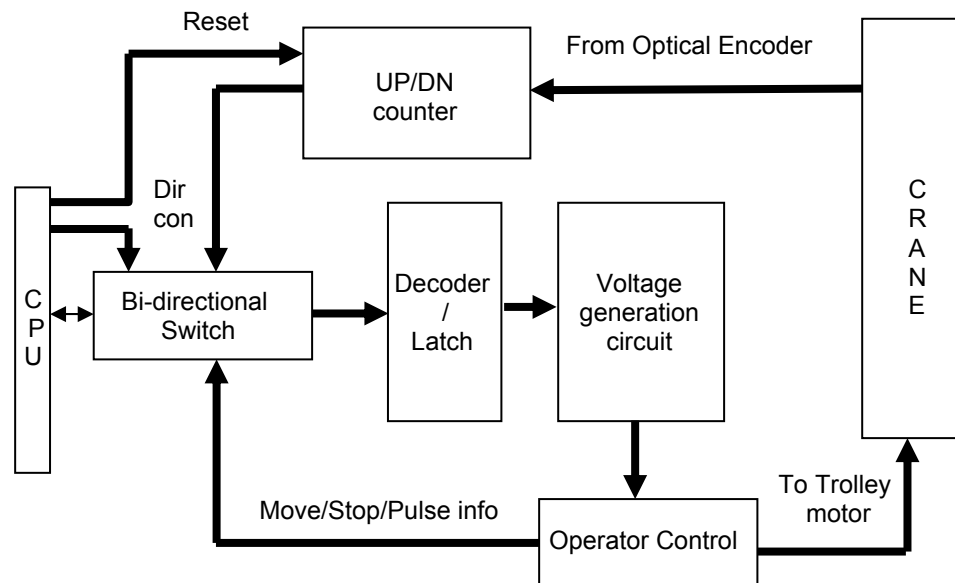


**Figure 3.3:-** Interconnection Block Diagram.

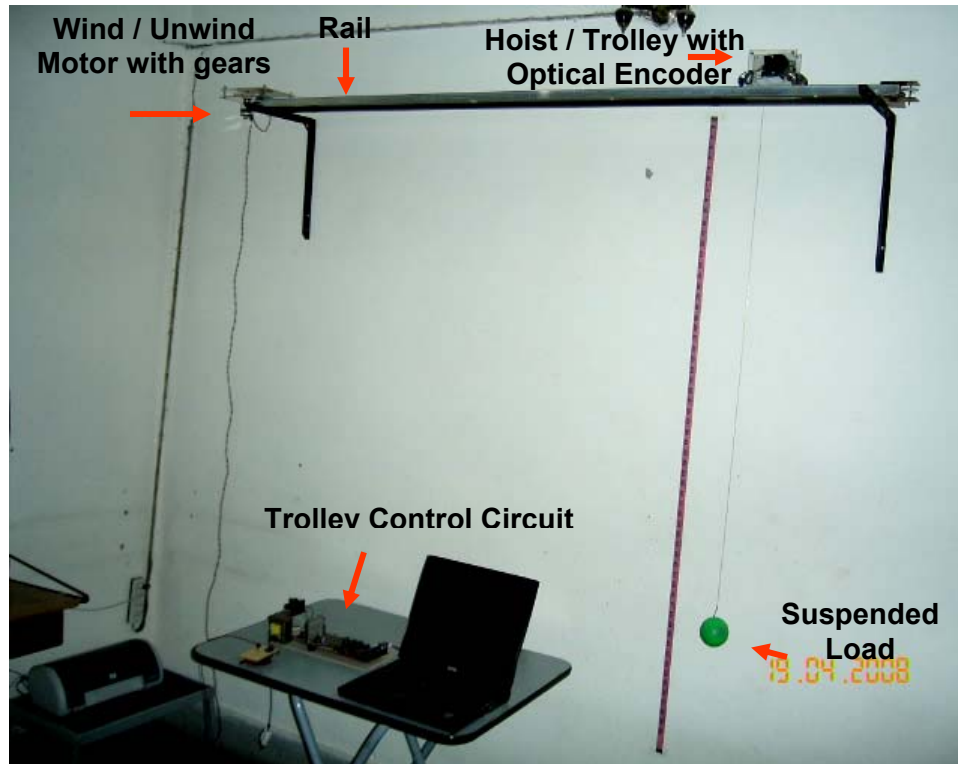


**Figure 3.4:-** Lab model of Crane.

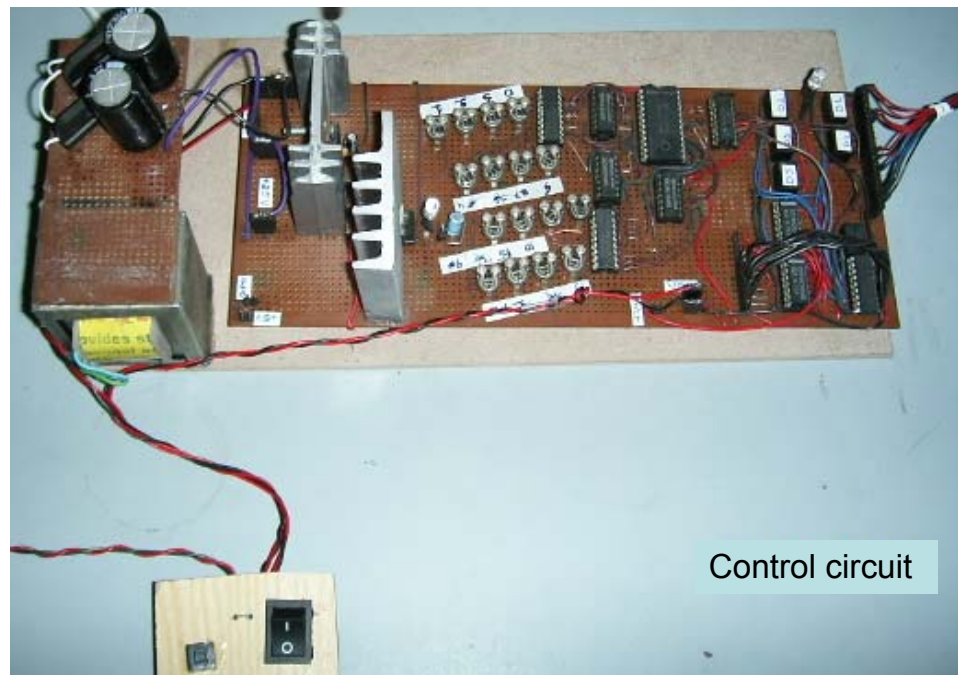


**Figure 3.5** Control circuit for generation of DC drive input for the motor to produce required acceleration.



### 3.3.2 For Inching Operation<sup>[14]</sup>

This method for dampening oscillations of a load supported by a crane relates to an open loop method for shaping the speed signal controlling the horizontal motion of a crane when inching or moving the crane a short distance. Again it is assumed that no other forces, except gravity and the carriage motor force are acting on the load. In particular, the load is not swinging at the beginning of a carriage run.

In a conventional open loop technique for load damping for inching operation, the acceleration rate is fixed. The period of load oscillation is determined. A request for a change in speed results in computing an acceleration time that will provide for half the requested speed change at the fixed acceleration rate. The fixed acceleration rate is applied to the motor for the determined acceleration time to provide half of the requested speed change and then followed by an equal interval of acceleration one-half period later to complete the requested speed change. Accelerations applied in this manner dampen load swing. Common feature of all such oscillation damping methods is that changes in speed commands cannot be instantly compensated. A certain settling time must elapse before speed changes are entirely compensated. The load oscillation dampener spread out the carriage accelerations over time to dampen oscillations. This produces an uncontrolled motion when the crane operator is trying to move the crane at a shorter distance. Once the operator has taken his finger off the control button to stop the crane, uncontrolled or erratic damping movements usually continue for a time. The existence of these uncontrolled damping movements makes it difficult for the operator to judge the final distance the crane will travel. Some operators accept this uncontrolled carriage motion and try to their best to anticipate the final displacement of the crane while others prefer to deactivate the load oscillation dampener during inching with an on-off switch and thereby avoid erratic damping movements.

In this method,  $T$  is determined and the drive signal comprising following three parts is generated and applied to the motor to cause carriage movement.

- a. The first part of the drive signal causes a carriage displacement as desired by the crane operator. This first part of the drive signal is generated in response to operator inching commands, such as pushing the forward directional button on a control pendant and releasing when the final destination is reached, causing the first part of the drive signal to end.
- b. The second part of the drive signal produces a carriage displacement opposite to that of the first part and is generated at a time  $T/6$  after the initiation of the first part of the drive signal. This part of the speed reference signal  $v(t)$  is the opposite of the first part of the speed reference signal  $v(t)$  but delayed by a time  $T/6$ . Specifically, the value of the speed reference signal  $v(t)$  for times between  $t_0+T/6$  and  $t_0+T/3$  is  $-v(t-T/6)$ . This causes the carriage to move back and return to its initial position.
- c. Finally, the third part of the drive signal is generated and applied to the motor drive. This third part of the speed signal is to be the same as of the first speed reference signal but delayed by  $T/3$  after the first part of the speed reference signal. Specifically, the value of the speed reference signal  $v(t)$  for times between  $t_0+T/3$  and  $t_0+T/2$  is  $v(t-T/3)$ , causing the carriage to return to the desired final position.

Carriage motion of this type i.e. a first motion, followed by an opposite second motion  $T/6$  later, and then followed by a third motion, the same as the first motion, but delayed by  $T/3$  after the first motion cause no extra displacement and so the final carriage destination is that displacement which was achieved at the end of the first part of the speed reference signal. The load oscillation dampener will automatically generate these second and third part of the speed reference signal  $v(t)$ . Advantage of the this method is that the sequence of motions will be executed even faster than the motions associated with the conventional open loop damping method, where two equal acceleration sequences are applied to the carriage a time  $T/2$  apart. In comparison, the time to complete the inching

sequence of this method is  $T/3$  plus the duration of the first part of the drive signal, while the aforementioned conventional open loop damping method would take  $T/2$  plus the duration of its first acceleration sequence.

### 3.4 Limitations

Although the method explained in this chapter are very effective and easily implement-able on existing old types of cranes and can be sufficient to the requirements of the most of the job but still have few major draw backs as explained under:-

- a. Being open loop method, it has been assumed that no external disturbances exist. However, in actual the effects of wind (especially on large gantry cranes) and effect of unstable platform (like cranes on ship) can not be ignored.
- b. It has also been assumed that there is no oscillation at the start of movement which may not be possible at many places. These systems have no remedy under such circumstances.
- c. If by the mistake of operator or some system error oscillations are developed in the process of traversing, operator has no procedure or control to suppress them, being open loop systems.
- d. As mentioned in the First method that operator sends a pulse well in advance of the destination point so that the reduction in speed should take place in the same fashion as it was increased, demands operator expertise in estimating the distance when he should send the pulse creates room for the mistake and so of damages.

In order to cater for these draw backs, in next chapter we will design a closed loop system by making use of newly emerging advance form of non linear control system technique i.e. Fuzzy Logic.

# Chapter 4

## Fuzzy Logic Controlled Crane

An introduction to fuzzy control logic is first presented after which detailed description of the crane controller design is given. Finally, simulation results of the controller are also presented to evaluate the performance.

### 4.1 Introduction to Fuzzy Logic<sup>[16]</sup>

Fuzzy logic is one of the recent developing methods in control that are gaining more popularity. The idea behind fuzzy logic is to write rules that will operate the controller in a heuristic manner, mainly in an (If A Then B) format. The arguments A and B are not exact numbers or equations, but they are descriptive words or phrases like small, big, cold, hot, high and very high etc. Any fuzzy controller consists of four main stages: Variable Fuzzification, Rules Application, Aggregation, and Defuzzification stages. These stages have many variations, so all the details mentioned later are specific to the design we have chosen. Starting with the Fuzzification stage, we map all of the crisp (numerical) values of the input variable into memberships in fuzzy logic sets. The whole crisp range is mapped into a number of fuzzy logic sets. The degree of membership for a certain numerical input depends on the shape of the fuzzy set and where does the crisp value lie in the range of this set. For example, in Figure 4.1, the variable  $\varphi = 1.25$  has 0.75 membership in Positive Small (**PS**) and 0.25 in Positive Medium (**PM**), while it has zero membership in the other sets. The shape of the membership functions is chosen to be triangular. Then, we apply the rules one at a time. If the antecedents of the rule are combined by an **AND** operator, then the minimum of all of the antecedent memberships is taken to be the membership of the output. But if they are combined by an **OR** operator, then the maximum membership is taken to be the output membership. After applying all of the fuzzy rules, the aggregation stage starts. At this stage, all of the outputs of the rules that belong to the same output variable are aggregated together. Summing all of

the outputs is the method chosen for this controller. Eventually, in the defuzzification stage, a crisp value is assigned for the output. Finding the centroid of the output shape is the method used here.

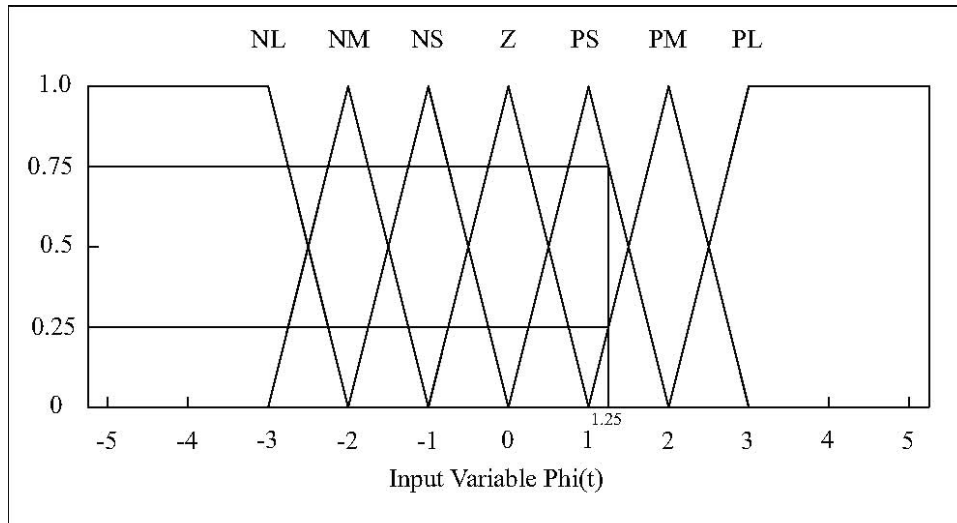


Figure 4.1: Example on fuzzy logic sets<sup>[16]</sup>.

## 4.2 Fuzzy Logic Controller Design

As shown in Figure 4.2, we start with the input signals from the operator. These

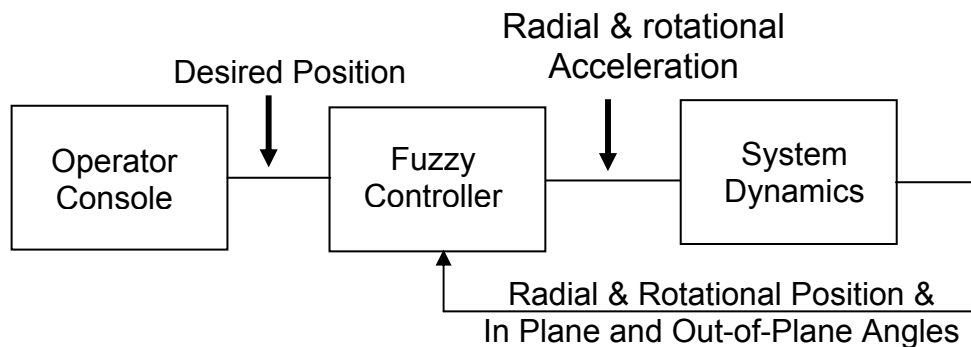
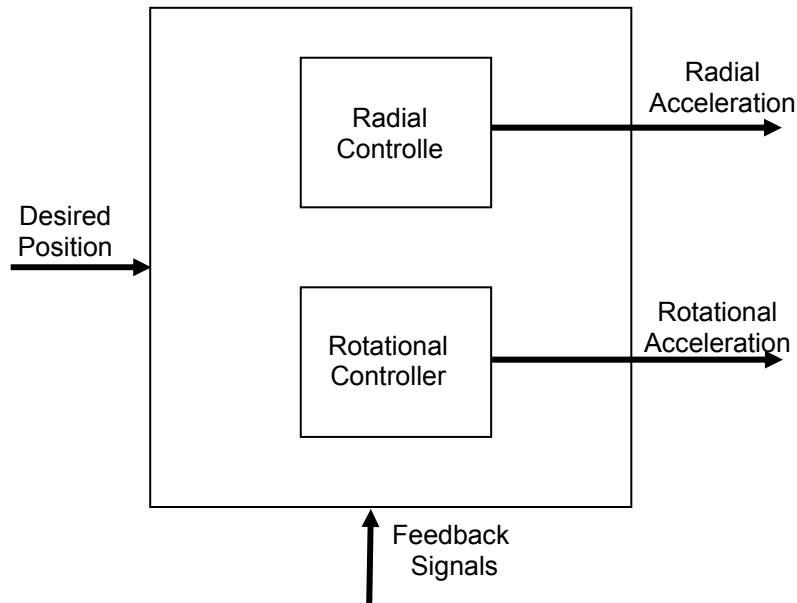


Figure 4.2: System block diagram with fuzzy logic controller.

Signals represent the desired radial position and rotational angle  $\gamma_d(t)$ . These two signals can be read from the operator's handle (joy stick). The fuzzy controller receives four other inputs from the feedback loop: the actual radial distance  $r_a(t)$ , the actual rotational angle  $\gamma_a(t)$ , the In-plane angle  $\phi(t)$ , and the

out-of-plane angle  $\theta(t)$ . The fuzzy logic controller (FLC) generates the radial and rotational accelerations, which are inputs to the system dynamics block. From Figure 4.3, it is clear that two separate controllers are employed. One is radial, which takes care of the transverse motion of the trolley over the jib; and the other is rotational, which handles the rotational motion of the jib.



**Figure 4.3:** Fuzzy logic control design.

Two fuzzy inference engines (FIE) are used inside each controller, shown in Figure 4.4.

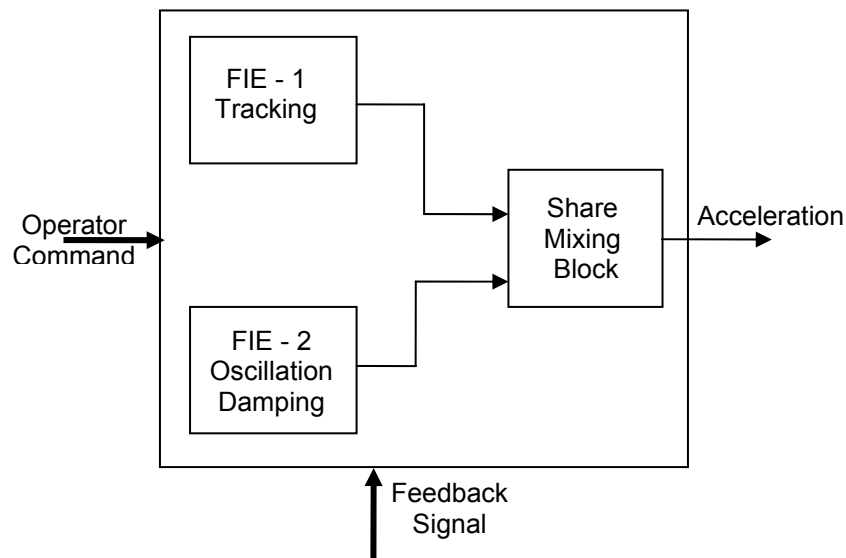


**Figure 4.4:** Two FIEs inside each FLC.

The first is the tracking FIE, which has the desired and actual radial distances as inputs for the radial controller and the desired and actual rotational angles as inputs for the rotational controller. Meanwhile the oscillations damping FIE has the In-plane angle  $\phi$  as an input for the radial controller and the out-of-plane angle  $\theta$  as inputs for the rotational controller. The outputs of the two FIEs are inputs to a variable-share mixing block, where the output from the tracking FIE is multiplied by a factor K and the oscillations damping FIE output is multiplied by (1-k). Then, these scaled outputs are added to obtain the controller output (acceleration). Through the design, the gain K is assigned a fixed value to obtain the optimal performance of the system. But it can be varied or it can be changed by the operator according to the current conditions of transportation. The output of the radial controller is  $\ddot{r}_{Reference}(t)$  and the output of the rotational controller is  $\ddot{\gamma}_{Reference}(t)$ . Next, we describe each controller and explain the fuzzy sets and rules in each FIE.

## 4.2.1 Radial Controller

This controller determines the radial acceleration of the trolley, which is fed to the system dynamics block to find the response. The outputs of the following FIEs are mixed with a gain  $K_{Radial} = 0.8$

### 4.2.1a Tracking FIE

This FIE has the actual radial distance  $r_a(t)$  and the desired radial distance  $r_d(t)$  and their derivatives  $\dot{r}_a(t)$  and  $\dot{r}_d(t)$ . Its output is  $\ddot{r}_{track}(t)$ . Before applying the fuzzy rules, we calculate two variables, the radial distance error  $E_r(t)$  and its derivative as follows:

$$E_r(t) = r_d(t) - r_a(t)$$

and 
$$\dot{E}_r(t) = \dot{r}_d(t) - \dot{r}_a(t)$$

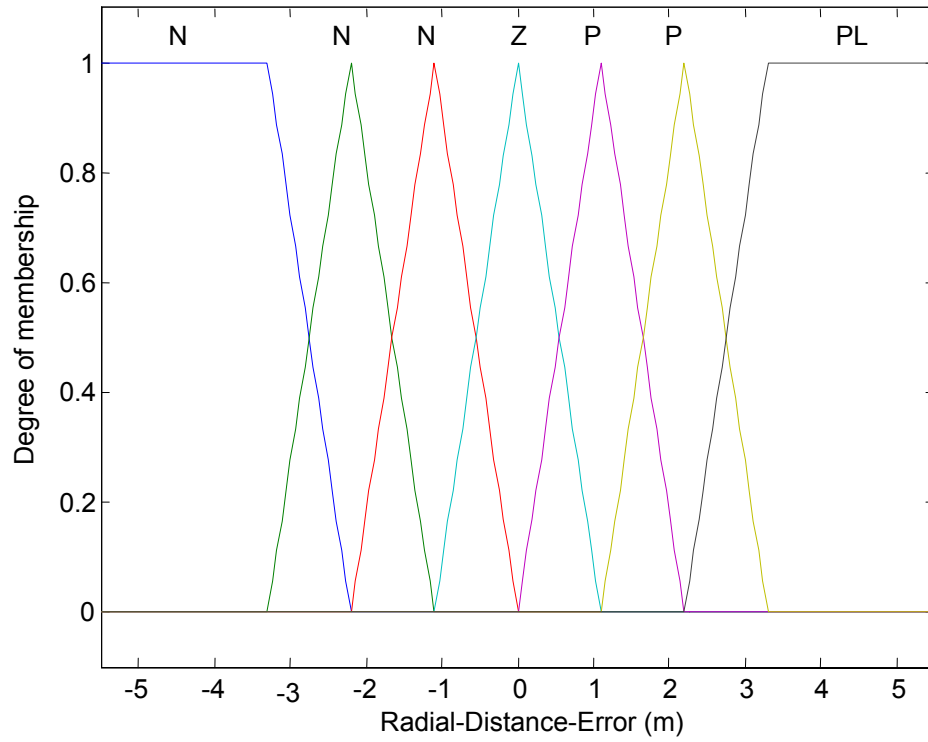


**Figure 4.5:** Fuzzification of  $E_r(t)$ .

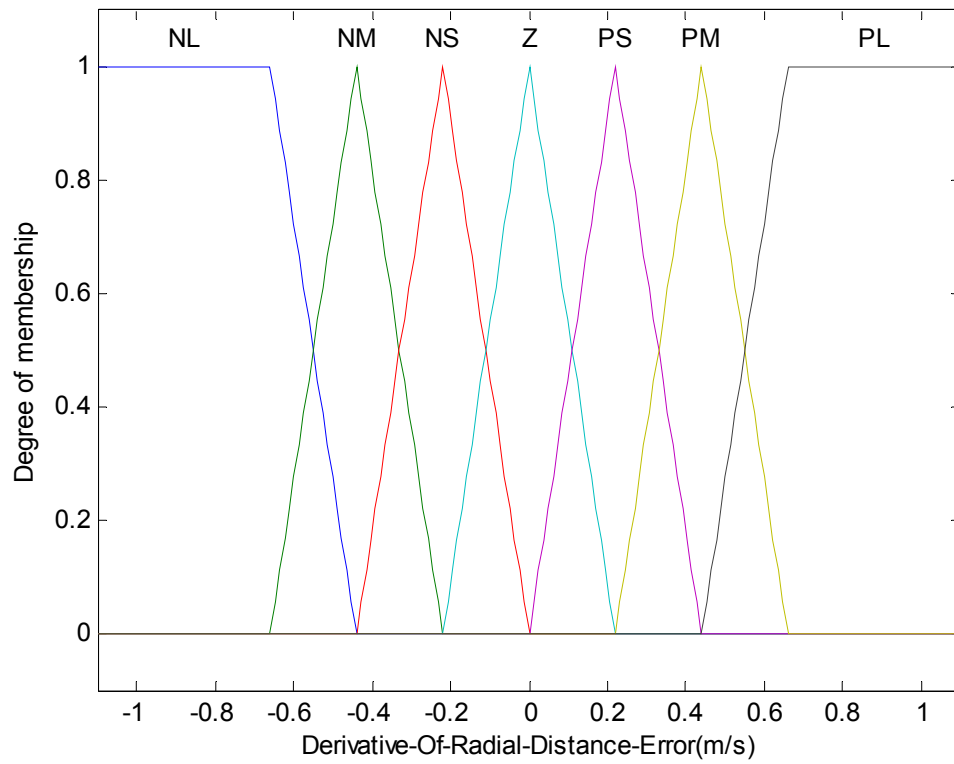


**Figure 4.6:** Fuzzification of  $\dot{E}_r(t)$ .



Then, they are fuzzified using the fuzzy sets shown in Figure 4.5 and Figure 4.6 and mapped on to output Fuzzy sets of Figure 4.7 to find  $\ddot{r}_{Track}(t)$ . Rules for mapping input variable to output are shown in Table 4.1. As a result of applying the rules, we have a fuzzy notion of the output variable  $\ddot{r}_{Track}(t)$ , which is transformed into a crisp value using the centroid method.

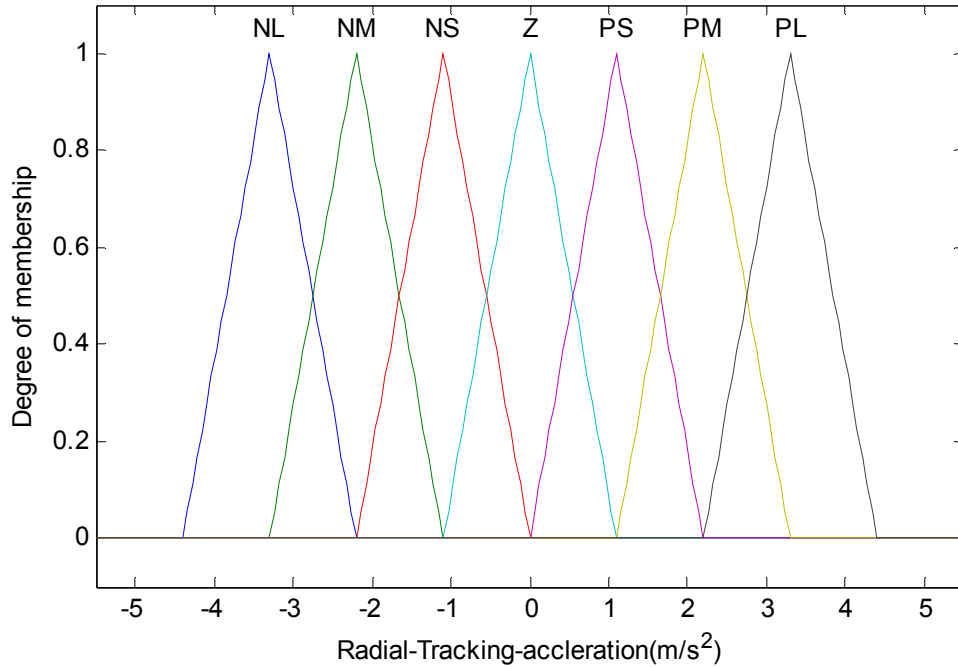


Figure 4.7 Fuzzy sets of  $\ddot{r}_{Track}(t)$ .

		DERIVATIVE OF RADIAL DISTRANCE ERROR						
		PL	PM	PS	Z	NS	NM	NL
RADIAL DISTANCE ERROR	PL	PL	PL	PM	PM	PS	PS	Z
	PM	PL	PM	PM	PS	PS	Z	NS
	PS	PM	PM	PS	PS	Z	NS	NS
	Z	PM	PS	PS	Z	NS	NS	NM
	NS	PS	PS	Z	NS	NS	NM	NM
	NM	PS	Z	NS	NS	NM	NM	NL
	NL	Z	NS	NS	NM	NM	NL	NL

Table 4.1: Rules for the radial tracking FIE.

### 4.2.1b Oscillations Damping FIE

In the oscillations damping FIE, the input variables are  $f(t)$  and  $\dot{f}(t)$ . The rules here are based on imitating a quarter-period delay controller. It tries to position the trolley over the load in order to damp any oscillations. The inputs to the FIE are fuzzified using the fuzzy sets shown in Figures 4.8 and 4.9. Similarly, the fuzzy rules in Table 4.2 are now applied to find the  $\ddot{r}_{Correction}(t)$ . After applying the rules, again we resort to defuzzify the output in order to find  $\ddot{r}_{Correction}(t)$ . Figure 4.10 shows the fuzzy sets of  $\ddot{r}_{Correction}(t)$ . Now, the output of this controller can be found by

$$\ddot{r}_{Reference}(t) = 0.8 * \ddot{r}_{Track}(t) + 0.2 * \ddot{r}_{Correction}(t)$$

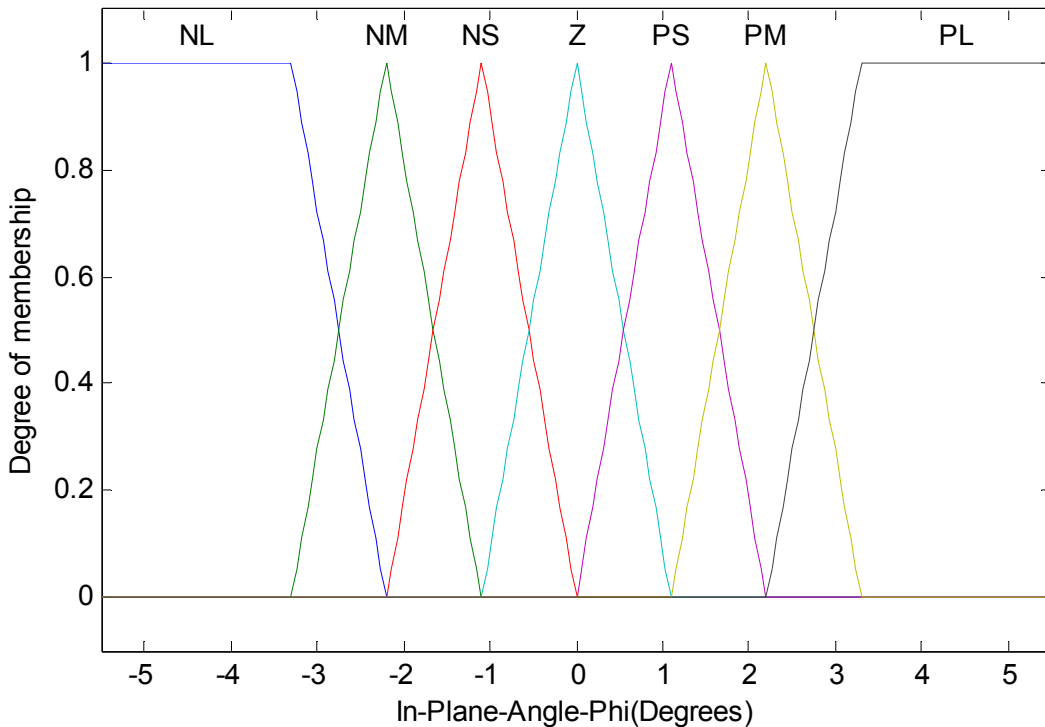
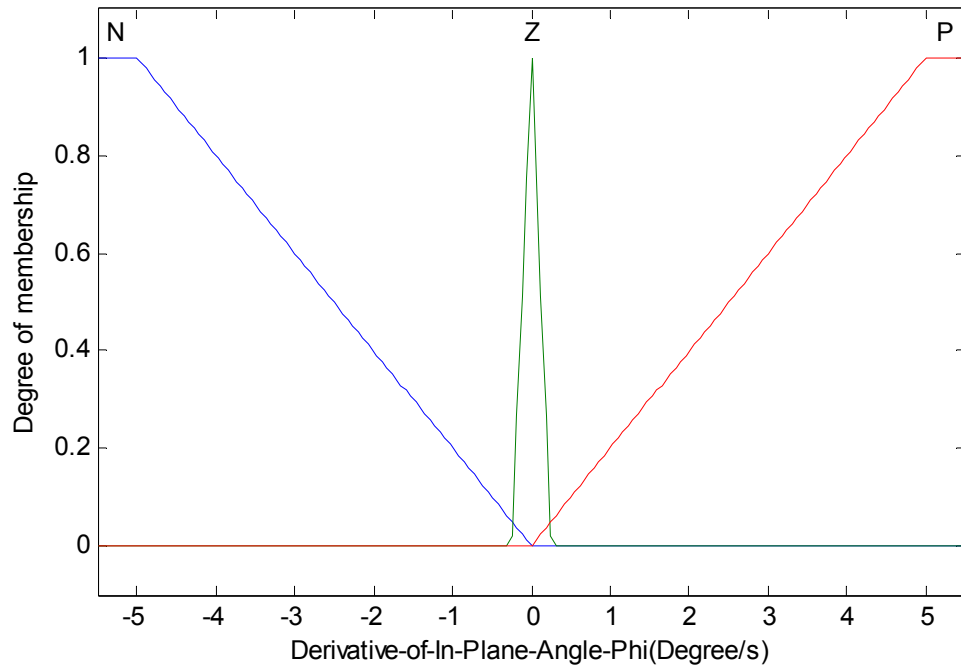
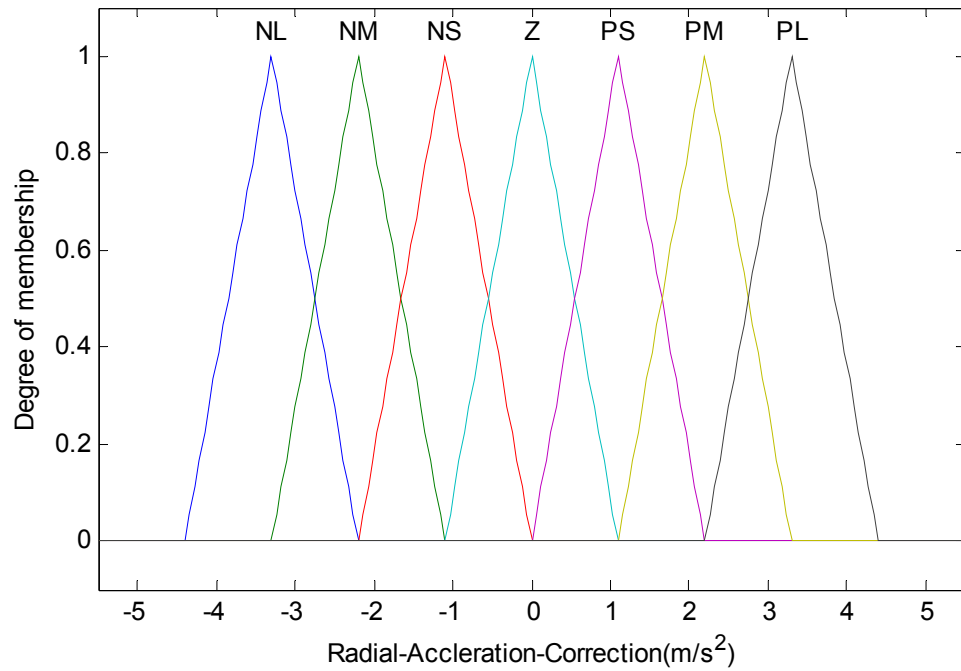


Figure 4.8: Fuzzification of  $f(t)$ .



**Figure 4.9:** Fuzzification of  $\dot{\phi}(t)$ .



**Figure 4.10:** Defuzzification of  $\ddot{r}_{Correction}(t)$ .

Derivative Of In-Plane Angle $\Phi(t)$	In- Plane Angle $\Phi(t)$							
		PL	PM	PS	Z	NS	NM	NL
	P	NL	NM	NS	Z	PS	PM	PL
	Z	Z	Z	Z	Z	Z	Z	Z
N	PL	PM	PS	Z	NS	NM	PL	

**Table 4.2:** Rules for the radial oscillations damping FIE.

## 4.2.2 Rotational Controller

Similar to the radial controller, the rotational controller consists also of two FIEs. It was found that the optimal value for the mixing gains is  $k_{Rotational} = 0.6$ . This lower value shows that it take more control action to damp the out-of-plane angle  $q(t)$  than the in-plane angle  $f(t)$ , which is expected because any attempt to reduce out-of-plane oscillations induces in-plane ones, thus causing more problems.

### 4.2.2a Tracking FIE

Here the FIE has the actual rotational angle  $g_a(t)$ , the desired rotational angle  $g_d(t)$ , and their derivatives  $\dot{g}_a(t)$  and  $\dot{g}_d(t)$ . The FIE output is  $\dot{g}_{Track}(t)$ . Before applying the fuzzy rules, we calculate two other variables, the rotational angle error  $E_g(t)$  and the derivative of the rotational angle error  $\dot{E}_g(t)$  as follows:

$$E_\gamma(t) = \gamma_d(t) - \gamma_a(t)$$

and

$$\dot{E}_\gamma(t) = \dot{\gamma}_d(t) - \dot{\gamma}_a(t)$$

Then they are fuzzified using the fuzzy sets shown in Figures 4.11 and 4.12. After that the rules in Table 4.3 are applied in order to find  $\hat{\theta}_{Track}(t)$  transformed

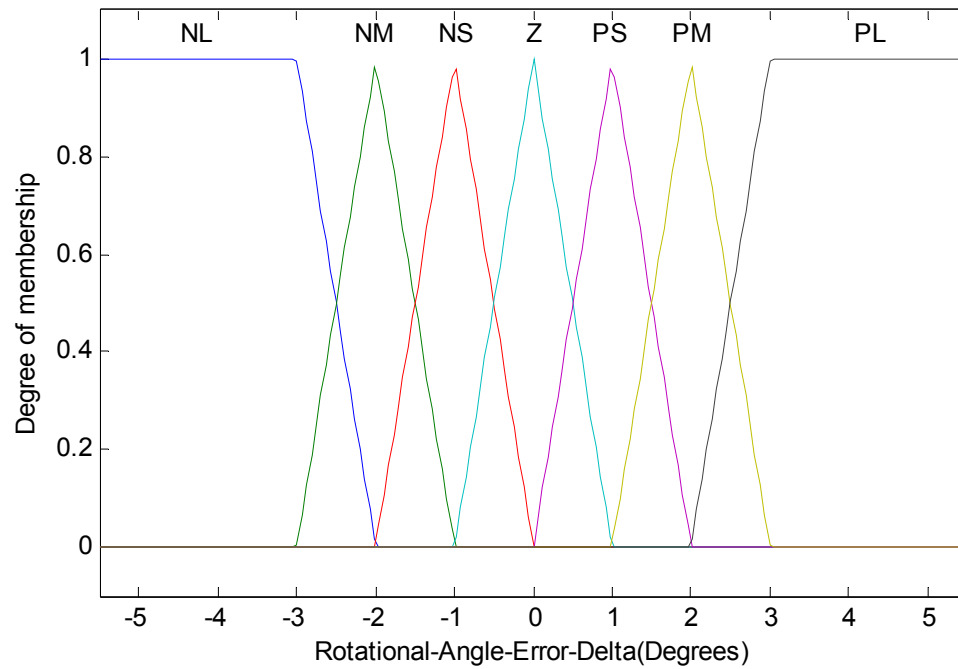


**Figure 4.11:** Fuzzification of  $E_g(t)$ .

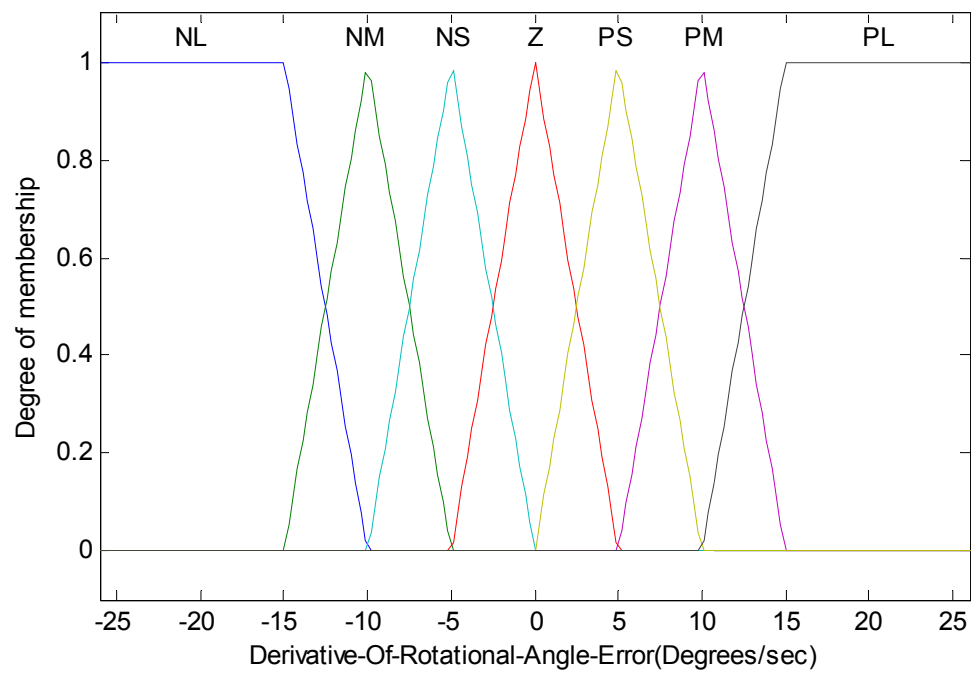


**Figure 4.12:** Fuzzification of  $\dot{E}_g(t)$ .

Into a crisp value using centroid method. Figure 4.13 shows the fuzzy sets of  $\hat{s}_{Track}(t)$ .

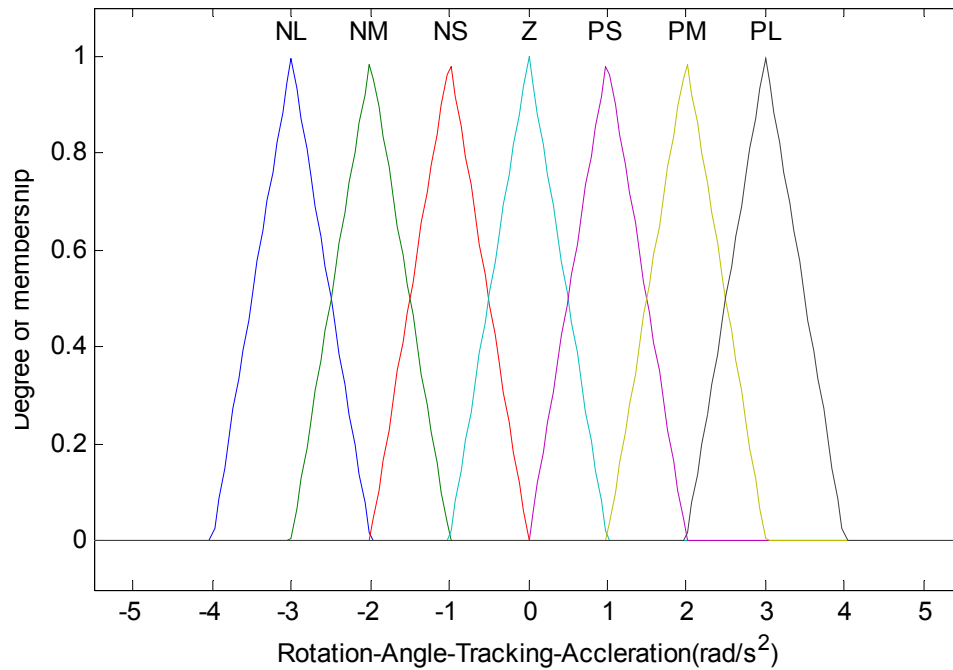


Figure 4.13: Defuzzification of  $\hat{s}_{Track}(t)$ .

ROTATIONAL ANGLE ERROR	DERIVATIVE OF ROTATIONAL ANGLE ERROR							
		PL	PM	PS	Z	NS	NM	NL
	PL	PL	PL	PM	PM	PS	PS	Z
	PM	PL	PM	PM	PS	PS	Z	NS
	PS	PM	PM	PS	PS	Z	NS	NS
	Z	PM	PS	PS	Z	NS	NS	NM
	NS	PS	PS	Z	NS	NS	NM	NM
	NM	PS	Z	NS	NS	NM	NM	NL
	NL	Z	NS	NS	NM	NM	NL	NL

Table 4.3: Rules for the rotational tracking FIE.

### 4.2.2b Oscillations Damping FIE

For the oscillations damping FIE, the input variables are  $q(t)$  and  $\dot{q}(t)$ . The rules here are based on the same concept used for the radial controller. The inputs to the FIE are fuzzified using the fuzzy sets shown in Figures 4.14 and 4.15. Fuzzy rules in Table 4.4 are now applied to find the  $\delta_{Correction}(t)$ . Finally, after applying the rules, we defuzzify the output in order to find  $\delta_{Track}(t)$ . Figure 4.16 shows the fuzzy sets of  $\delta_{Correction}(t)$ . Now, the output of this controller can be found according to

$$\ddot{\gamma}_{Reference}(t) = 0.6 * \ddot{\gamma}_{Track}(t) + 0.4 * \ddot{\gamma}_{Correction}(t)$$

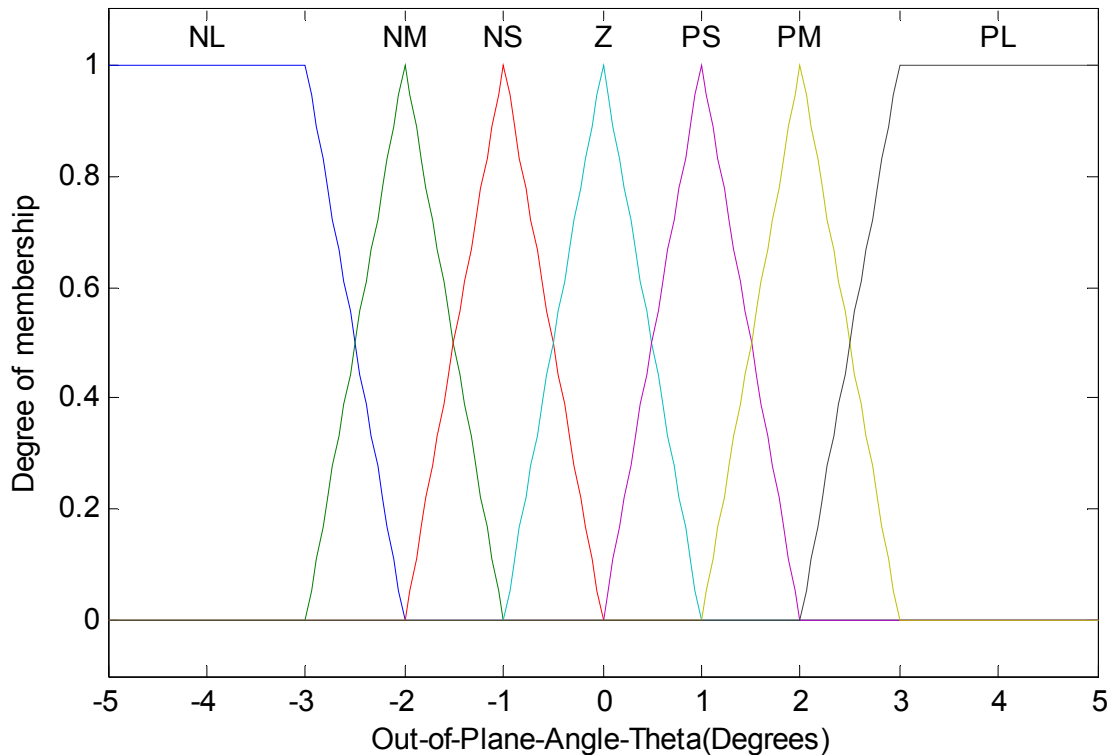
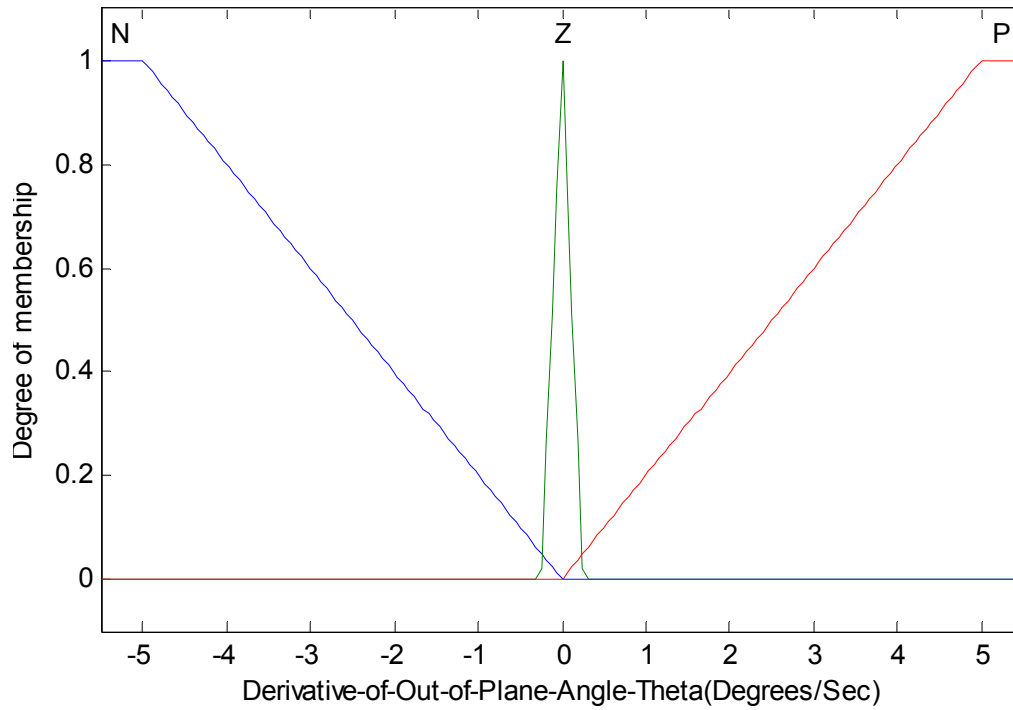


Figure 4.14: Fuzzification of  $q(t)$ .



**Figure 4.15:** Fuzzification of  $\dot{\theta}(t)$ .

Derivative Of In-Plane Angle $\theta(t)$	Out- of- Plane Angle $\theta(t)$							
		PL	PM	PS	Z	NS	NM	NL
P		PL	PM	PS	Z	NS	NM	NL
Z		Z	Z	Z	Z	Z	Z	Z
N		PL	PM	PS	Z	NS	NM	NL

**Table 4.4:** Rules for the rotational oscillations damping FIE.



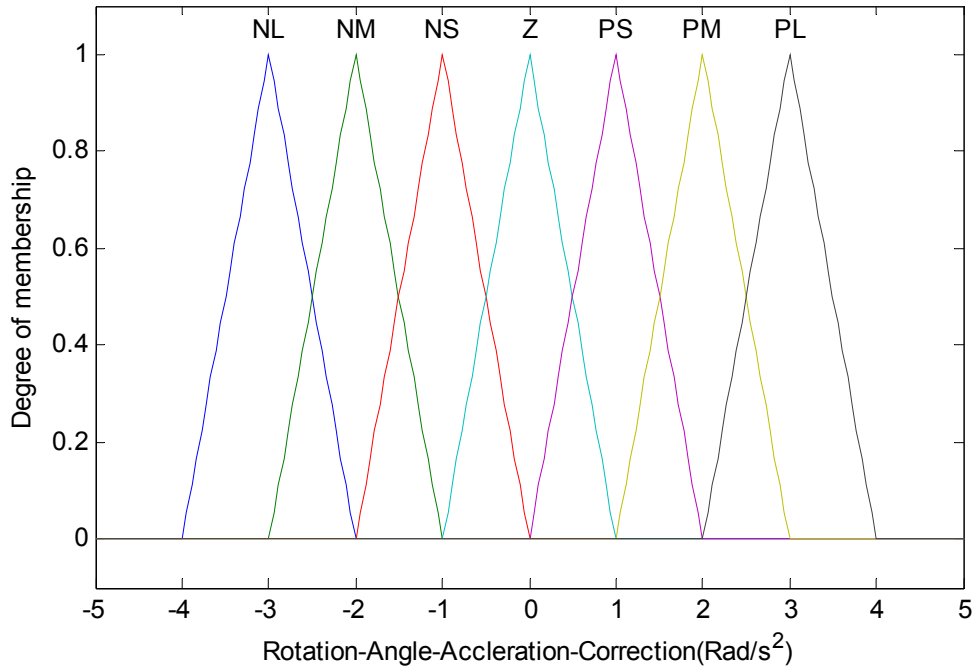


**Figure 4.16:** Defuzzification of  $\delta_{Correction}(t)$ .

### 4.3 Simulation Results

In order to test the performance of the designed controller, we used the MATLAB software<sup>[13]</sup> and its Fuzzy Logic Toolbox<sup>[16]</sup>. The toolbox provided a friendly Graphical User Interface (GUI), which made the testing faster and more efficient. The first step in testing the controller was to build the simulation model and generate an operator signal for testing which was executed as given below.

#### 4.3.1 Radial Case

In this case, the cable length is set equal to 1.0 m, and the trolley is moved radially 0.75 m from  $r = 0.25$  m to  $r = 1.0$  m. The trolley accelerates for 3/8th of the cable period i.e. 0.75 sec, moves at a constant velocity of 0.23078 m/sec for 2.5 sec, and decelerates for another 0.75 sec, Figure 4.17. The whole operation is executed within 4.0 sec. The acceleration amplitude is  $0.3077$  m/sec<sup>2</sup>.

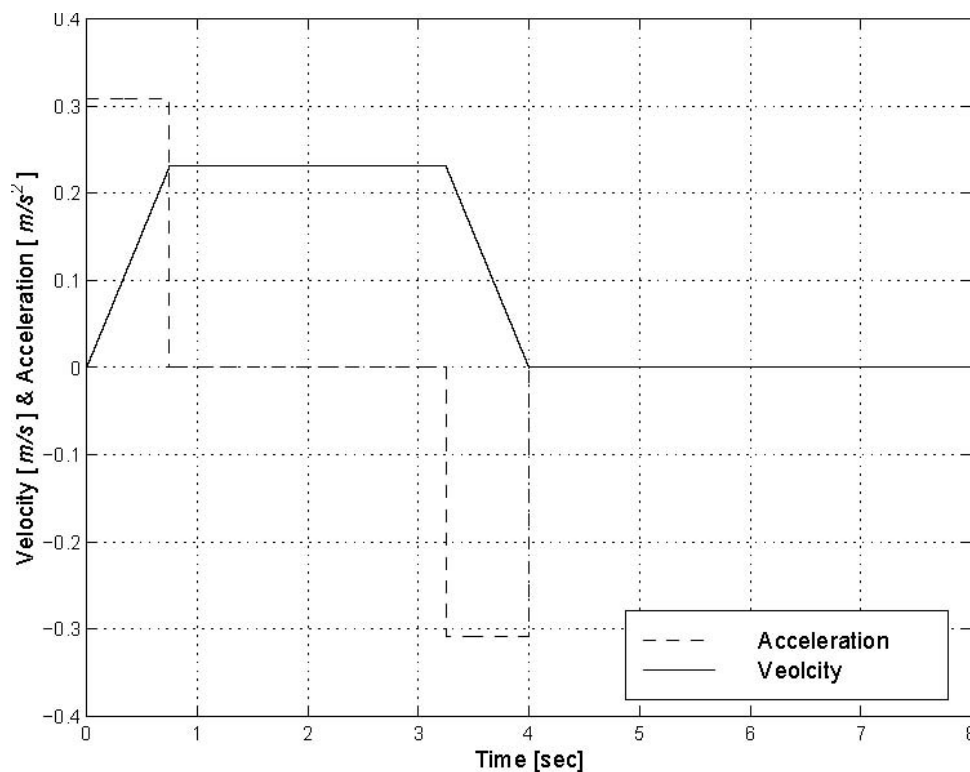
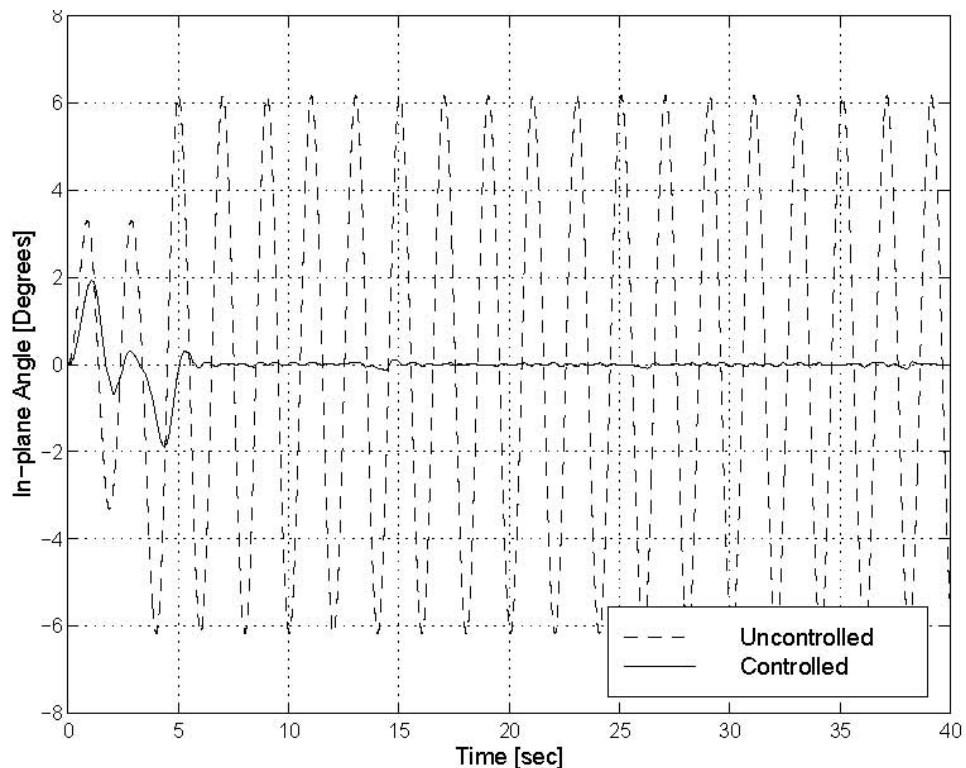


Figure 4.17: Operator radial signal.

In Figure 4.18, we compare the controlled and uncontrolled in-plane oscillation angle generated as a result of given input. In the uncontrolled response, the

oscillations continue with amplitude of  $6^\circ$  without any damping. In fact, the uncontrolled payload oscillates with amplitude of  $3^\circ$  after the acceleration period. When the deceleration occurs, it adds more energy to the payload oscillations, thereby raising the amplitude of oscillations to  $6^\circ$ . We note that the initial kick of the in-plane angle is less than  $2^\circ$  during the acceleration phase and about  $-2^\circ$  during the deceleration phase. Also, we note that the oscillations are damped within about 5 sec. The controller has no effect on the rotational angle  $g(t)$  or the out-of-plane oscillation angle  $\theta(t)$ . We also note that it takes about



**Figure 4.18:** Uncontrolled Vs controlled in-plane oscillation angle  $f(t)$  for the radial case using the fuzzy controller.

15sec for the trolley to reach the end position, even though the oscillations are damped within 5sec. Figure 4.19 shows both the trolley desired position commanded by the operator and the actual position. The overshoot in the trolley position is somewhat large, about 7cm. The trolley lags the operator command at the beginning and then catches up with an under-damped response. We note

that the steady-state error is zero. So we conclude that the performance of the controller is good.

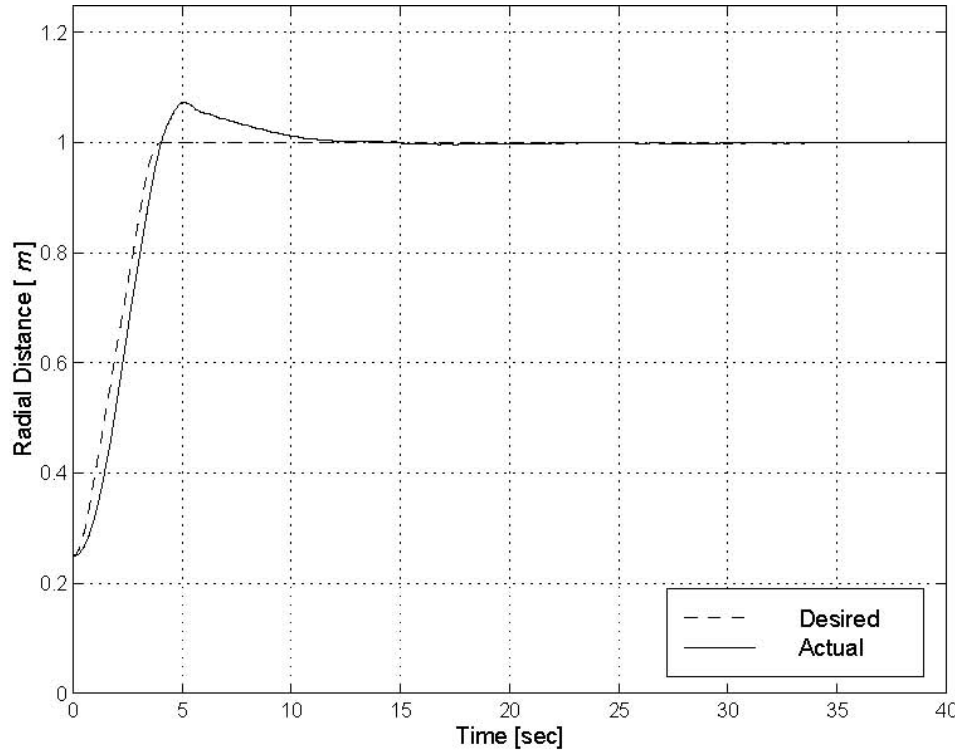


**Figure 4.19:** Desired and actual radial distances for the radial case using the fuzzy controller.

### 4.3.2 Rotational Case

For this case, the cable length is also set equal to 1.0 m, the jib is rotated 90° from its initial position, and the trolley is set 1.0 m away from the center to magnify any oscillations due to the rotational motion. The jib rotates with an acceleration of 0.4928 rad/s<sup>2</sup> for 0.75sec, with a constant angular velocity of 0.3696 rad/s for 3.8sec, and then decelerates for another 0.75sec, Figure 4.20 shows the signal. The whole operation takes 5 sec. In Figures 4.21 and 4.22, we compare the controlled and the uncontrolled in-plane and out-of-plane angles. In the uncontrolled case, initially the in-plane angle increases slightly because the motion starts perpendicular to the jib plane, then the in-plane angle increases to more than 3.5° during the constant angular velocity phase due to the centrifugal force. Finally, the in-plane angle undergoes a persistent oscillation of more than

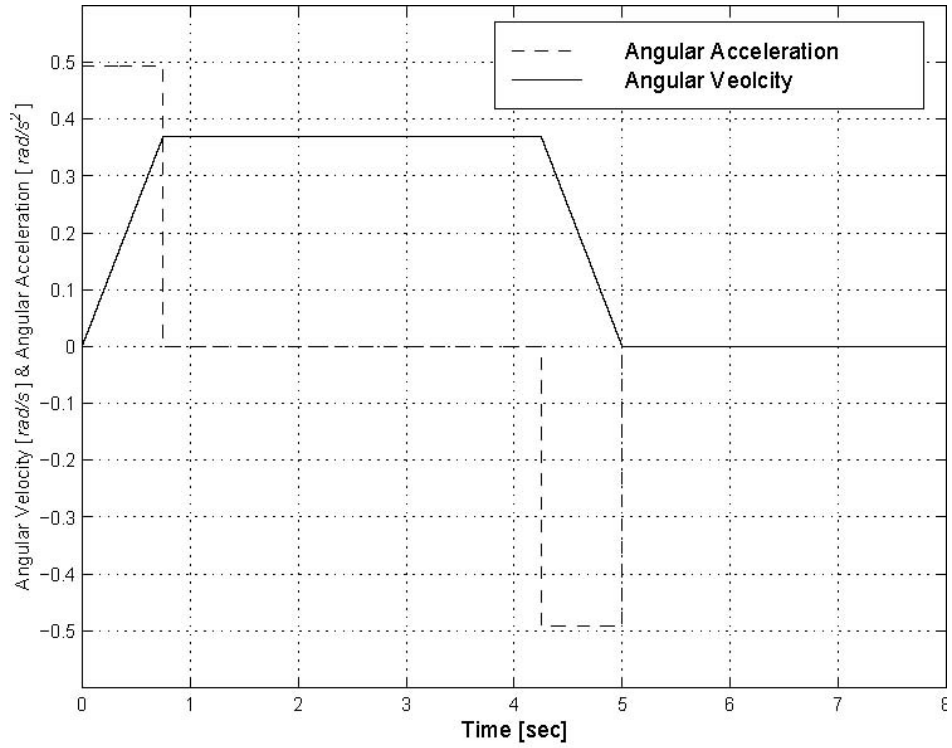


**Figure 4.20:** Operator rotational signal.

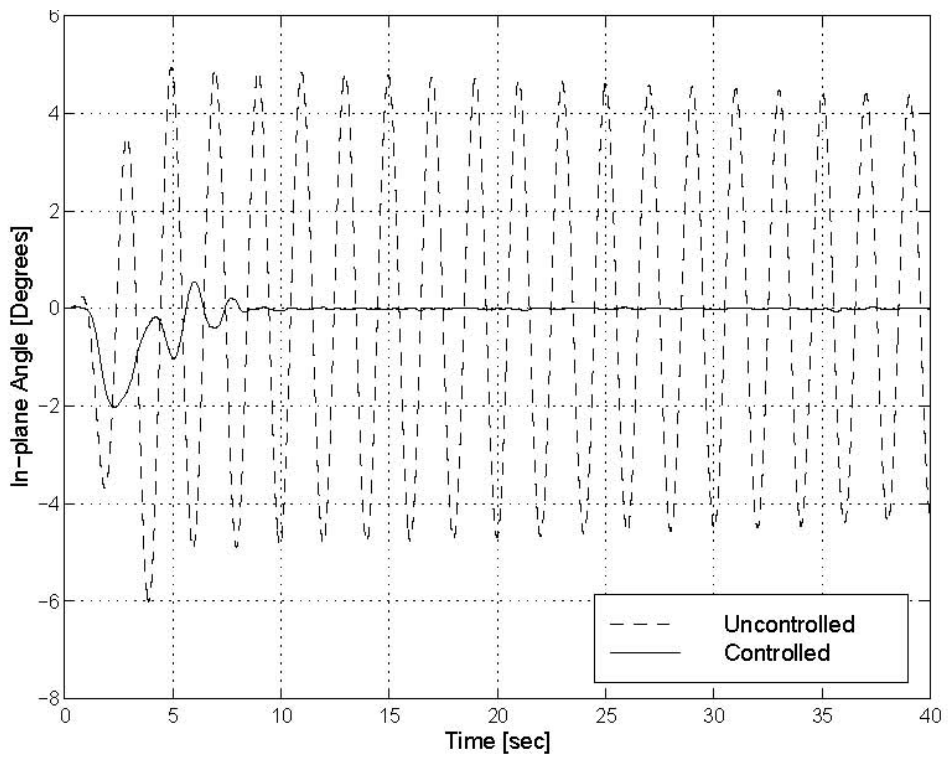


**Figure 4.21:** Uncontrolled Vs controlled in-plane oscillation angle  $f(t)$  for the rotational case using the fuzzy controller.

4°. On the other hand, the out-of-plane angle increases to more than 4.5° in the acceleration phase and persists afterward. There is a continuous energy exchange between the in-plane and out-of-plane motions, resulting from a one-to-one internal resonance between these modes. Closing the loop results in a decrease in both the in-plane and out-of-plane motions. The in-plane angle reaches -2° before it decays to almost zero in 10s. On the other hand, the out-of-plane angle increases to approximately 4° before it decays to almost zero in 25s. We see from Figures 4.22 to 4.23 that it takes about 20s to reach the final

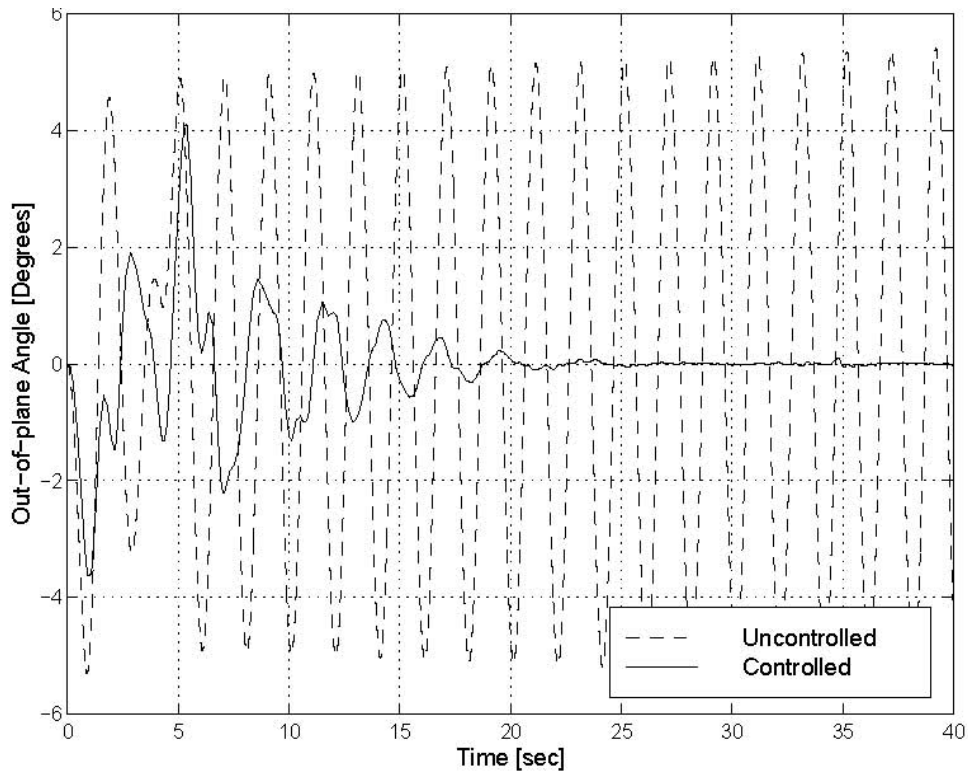


**Figure 4.22:** Uncontrolled Vs controlled out-of-plane oscillation angle  $\theta(t)$  for the rotational case using the fuzzy controller.

state and to reduce the oscillation angles almost to zero which is very long for such a small input signal. In order to damp the oscillations in the in-plane angle, the trolley needs to be moved about 10cm ahead from its initial position, which is considered to be a large deviation. As for the rotational angle of the jib, it has experienced a moderate overshoot of about 7° as shown in Figure 4.24. So even though the controller showed good performance in keeping the oscillation angles small, the time of the maneuver is somewhat large.

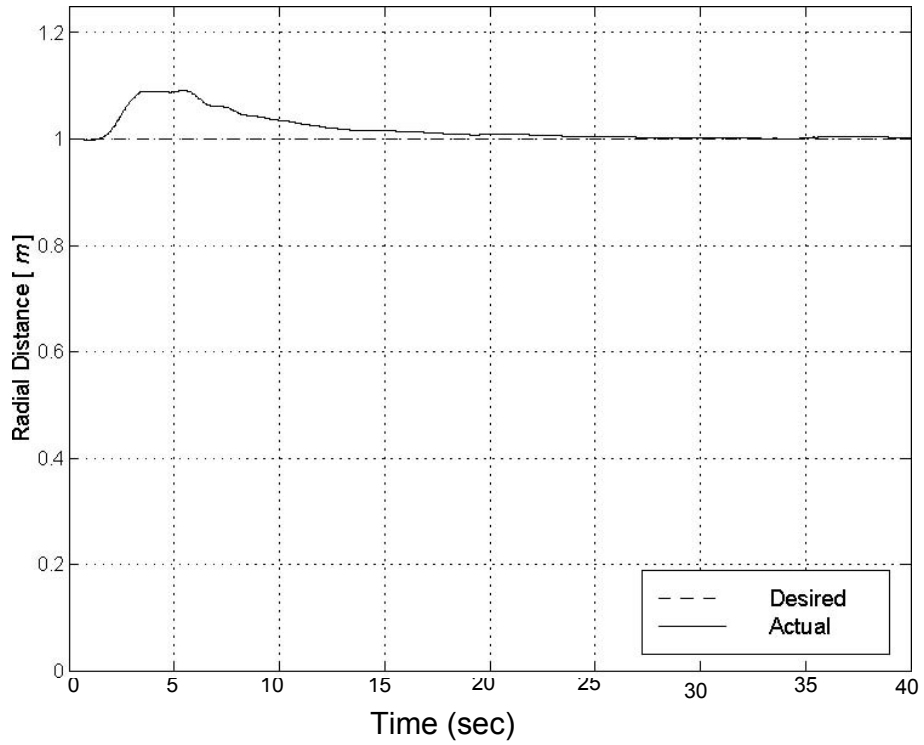


**Figure 4.23:** Desired and actual radial distances for the rotational case using the fuzzy controller.

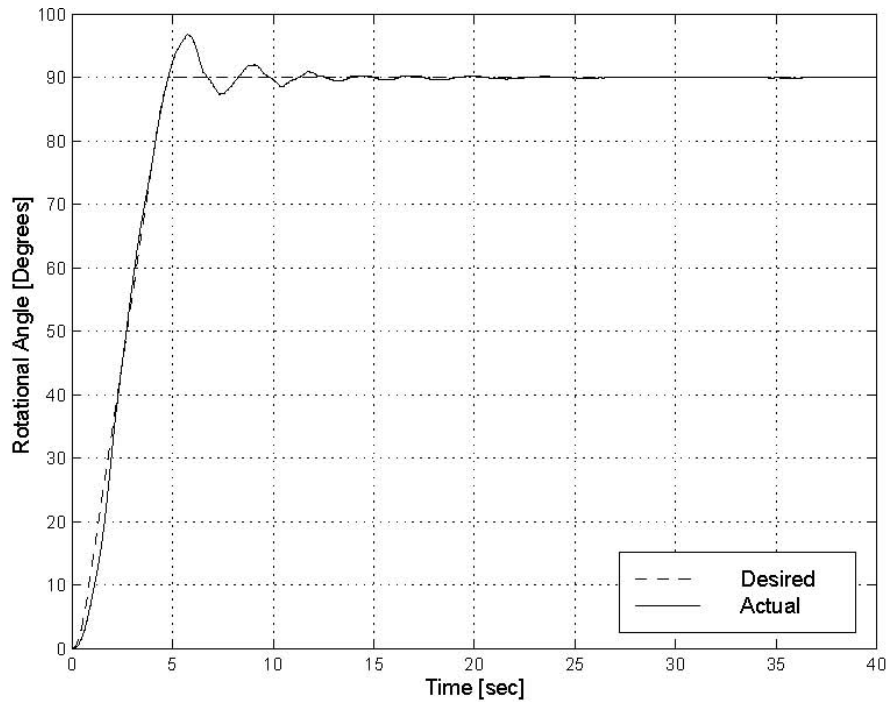


**Figure 4.24:** Desired and actual rotational angles for the rotational case using the fuzzy controller.

### 4.3.3 Compound Case

In this case, a combination of the radial and rotational motions is applied. The trolley is moved on the jib a distance of 0.75m as in the radial case, while the jib is rotated  $90^\circ$  around the tower as in the rotational case. We compare in Figures 4.25 and 4.26 the controlled and uncontrolled in-plane and out-of-plane angles. Again, in the uncontrolled case, energy is being continuously exchanged between the two modes of oscillations due to the one-to-one internal resonance between them. The in-plane angle grows to more than  $7^\circ$  in 40 sec, whereas the out-of-plane angle reaches more than  $9^\circ$  in 5sec. Figures 4.25 and 4.26 show that the oscillation period of the payload is 2 sec. Closing the loop results in a significant reduction in both angles. The in-plane angle grows to about  $2.5^\circ$  in the deceleration period, but it then decreases to almost zero within 10 sec. On the other hand, the out-of-plane angle increases initially to almost  $5^\circ$  before it decays to almost zero in 25 sec. This settling time is considered long for such a small model.

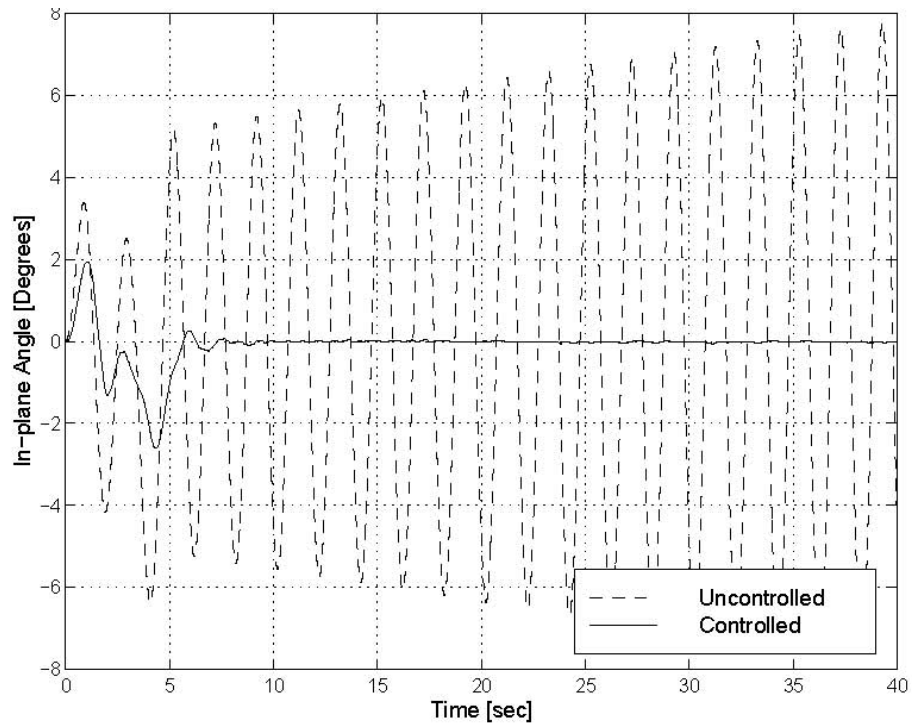


**Figure 4.25:** Uncontrolled Vs controlled in-plane oscillation angle  $f(t)$  for the compound case using the fuzzy controller.



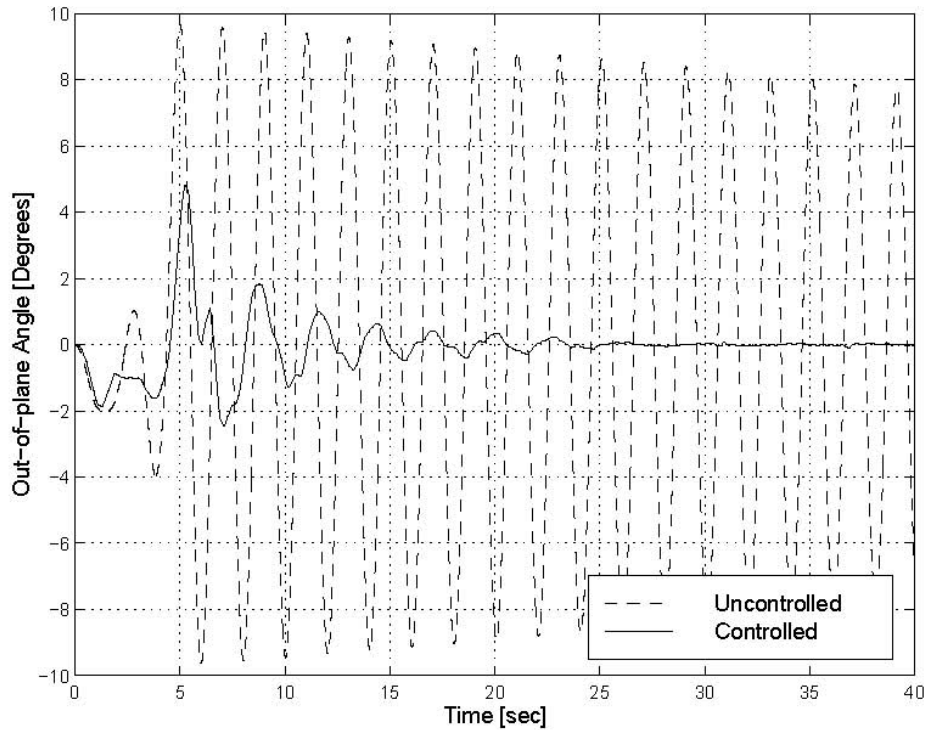


**Figure 4.26:** Uncontrolled Vs controlled out-of-plane oscillation angle  $\theta(t)$  for the compound case using the fuzzy controller.

Figure 4.27 shows the radial distance of the trolley on the jib. A problem that is clear here is that the overshoot is large, about 20 cm. With this large overshoot, the trolley takes more than 15 sec to reach its end position, which is a long time for such a small drive signal. As for the rotational angle of the jib, its overshoot is reasonable, about  $8^\circ$ . But Figure 4.28 shows that it also takes a long time to settle like the trolley i.e. about 12 sec.

#### 4.3.4 Damping Case

In this case, we investigate the effectiveness of the controller to damp initial disturbances. We started with an initial disturbance of  $75^\circ$  for each of the oscillation angles  $q(t)$  and  $f(t)$ . The trolley is placed at a distance of 1.0 m on

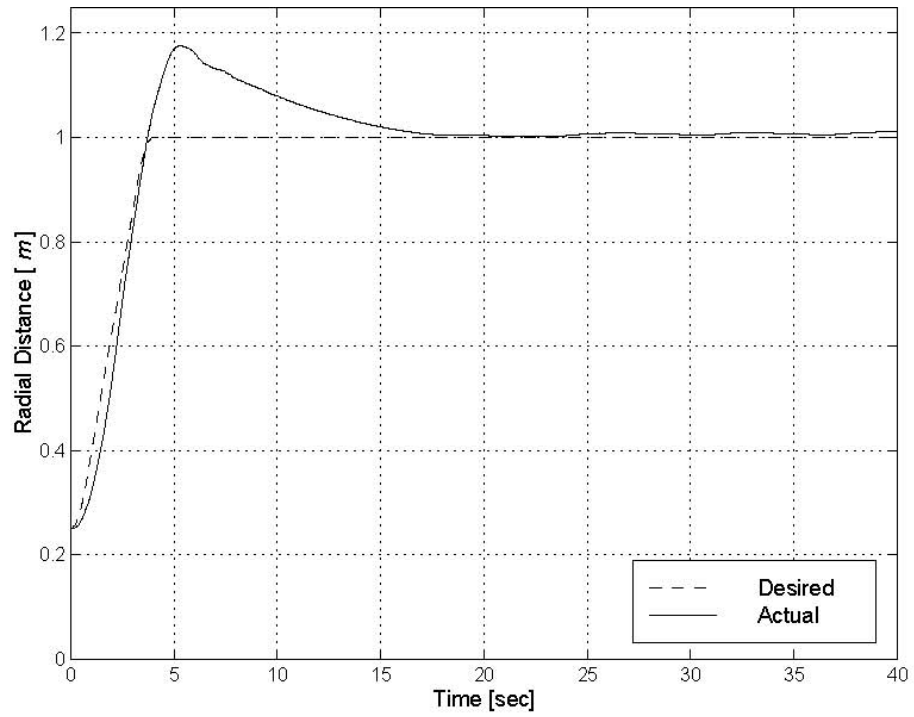


**Figure 4.27:** Desired and actual radial distances for the compound case using the fuzzy controller.

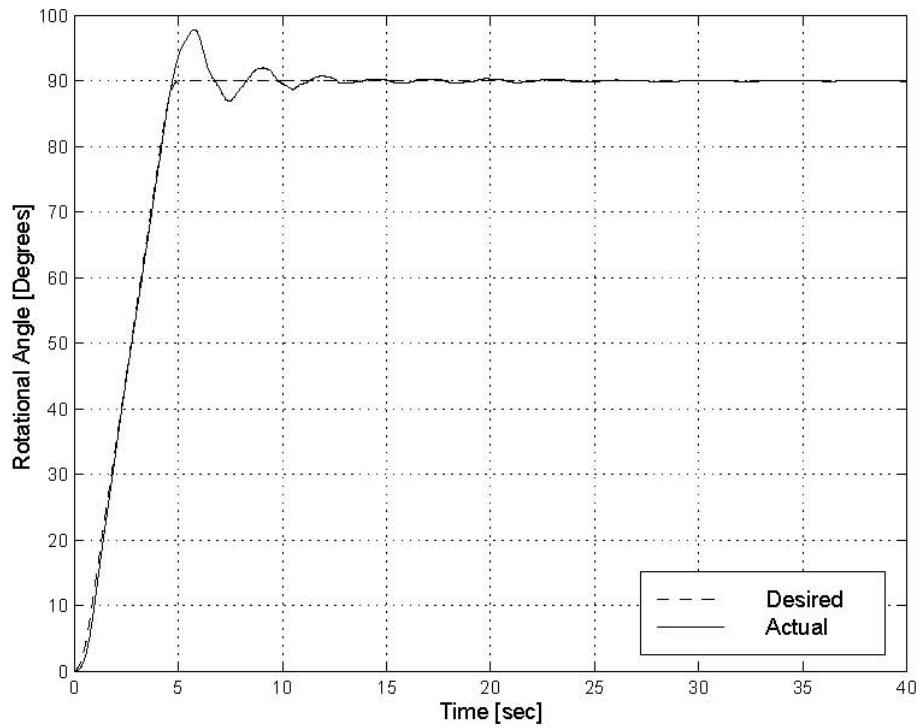


**Figure 4.28:** Desired and actual rotational angles for the compound case using the fuzzy controller.

the jib to magnify the oscillations effect. In Figures 4.29 and 4.30, we compare the controlled and uncontrolled in-plane and out-of-plane motions. Because the model does not include damping, the uncontrolled angle continue to oscillate

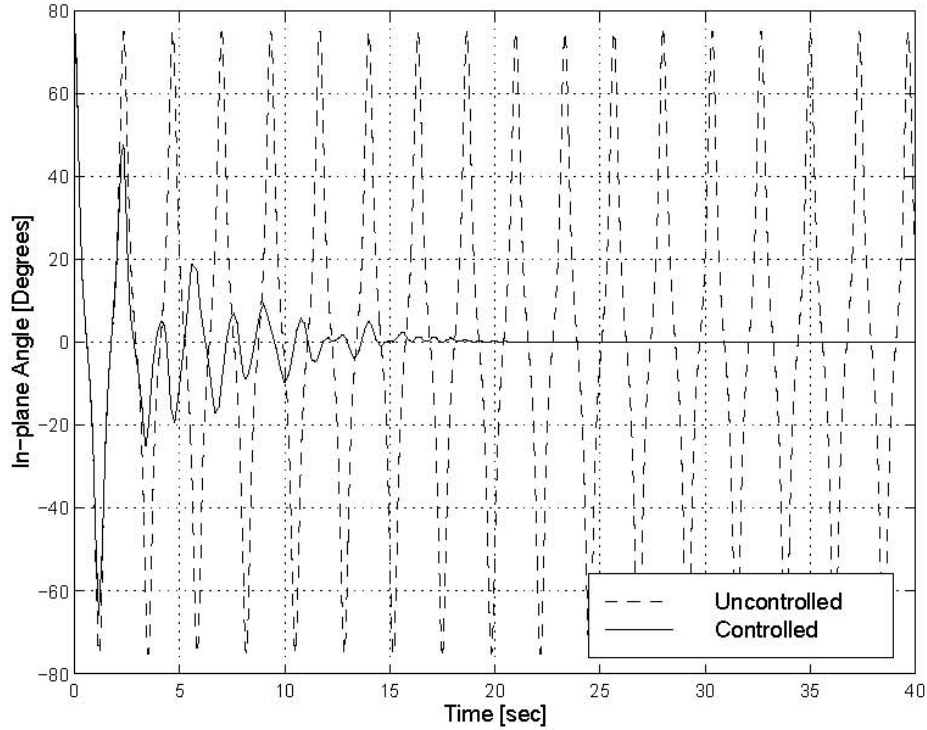


**Figure 4.29:** Uncontrolled Vs controlled in-plane oscillation angle  $\phi(t)$  for the damping case using the fuzzy controller.

with amplitude of  $75^\circ$  for long. On the other hand, applying the controller, we find that the in-plane motion decays below  $10^\circ$  after 8 sec and to almost zero within 20 s. In contrast, the damping of the out-of-plane motion is much slower. It takes about 18 s for this motion to decay below  $10^\circ$  and it takes about 25 sec for it to decay to almost zero.

In Figures 4.31 and 4.32, show the deviations of the trolley position and the rotational angle of the jib from their desired values. The maximum deviation of the trolley from the desired distance (1.0 m) is about 10 cm, which is small. Moreover, the maximum swing of the rotational angle of the jib to damp the oscillations is less than  $10^\circ$ , which is also considered to be small. Even though the time taken to damp these large initial disturbances is somewhat long, the trolley and jib deviations needed to damp these oscillations are considered to be small.

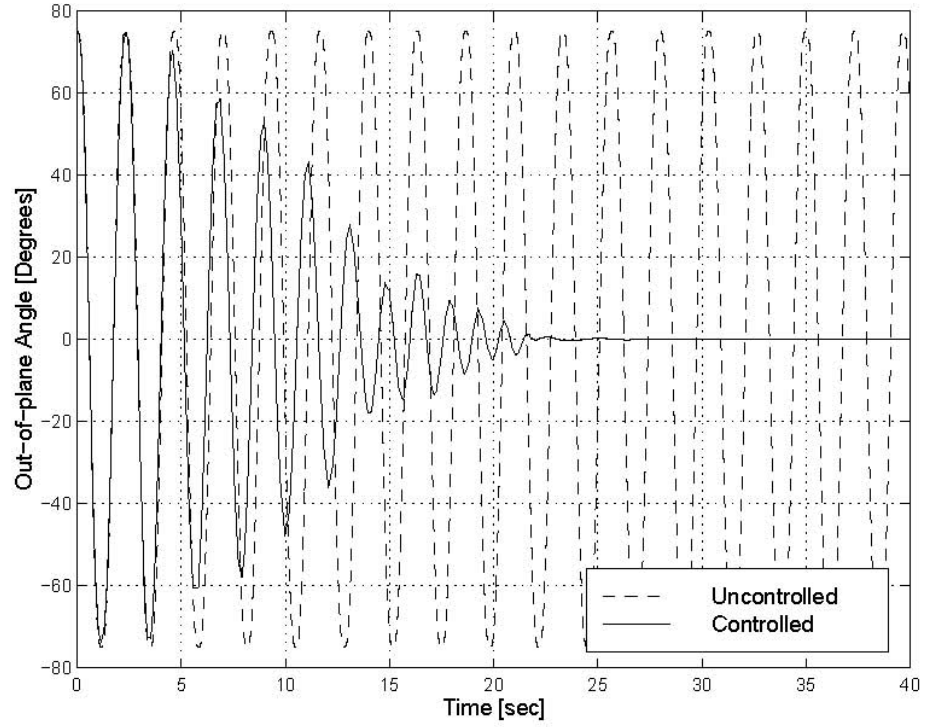


**Figure 4.30:** Uncontrolled Vs controlled out-of-plane oscillation angle  $\theta(t)$  for the damping case using the fuzzy controller.

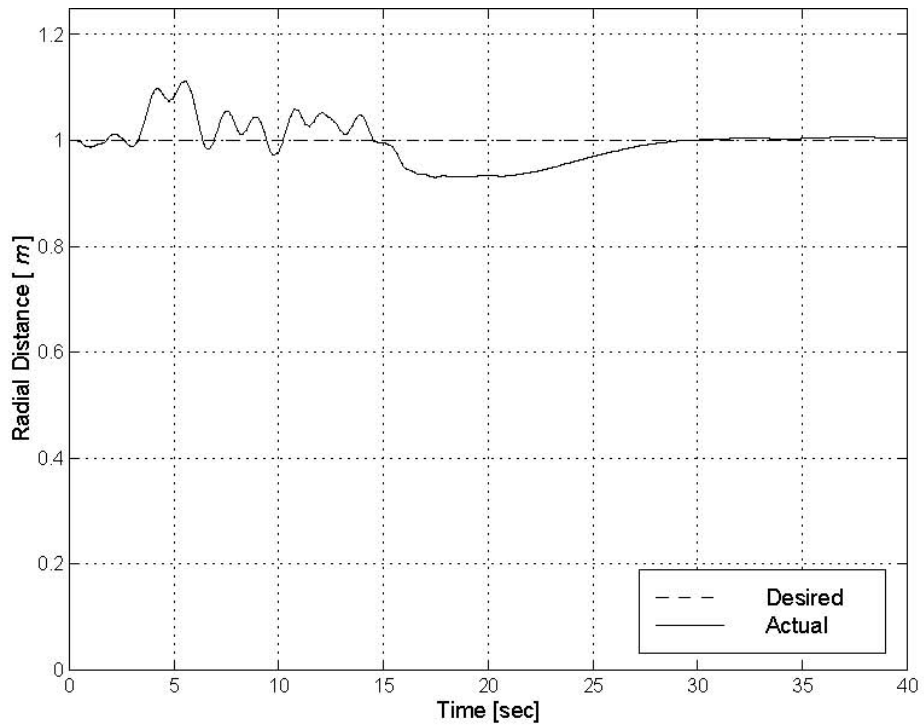


**Figure 4.31:** Desired and actual radial distances for the damping case using the fuzzy controller.

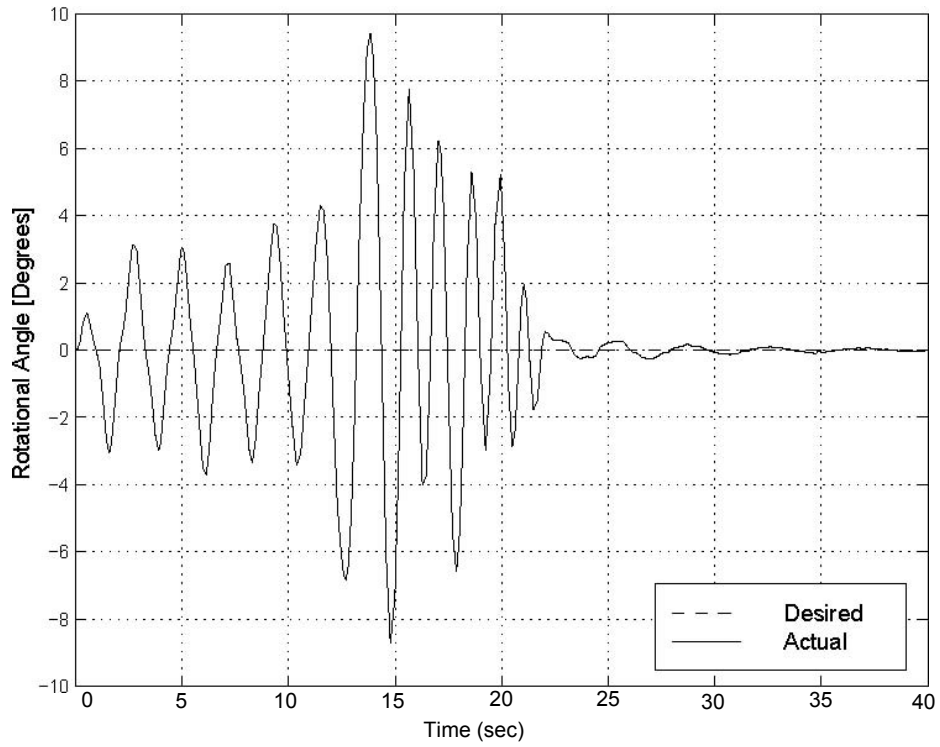


**Figure 4.32:** Desired and actual rotational angles for the damping case using the fuzzy controller.

This gives the fuzzy logic controller an advantage in cases where the trolley or the jib can not be moved as fast and the damping time is not important.

# CHAPTER 5

## Conclusion and Recommendations

### 5.1 Conclusions

In this research paper we designed two types of controllers. These controllers were designed to control the motion of the crane and reduce the payload oscillations. The first controller is open loop controller which assumes no initial and external disturbance. This type of controller is designed just by considering the characteristics of pendulum with flexible pivot. Practical demonstration of the concept is also demonstrated on a developed model crane. Although the oscillation damping methods explained in chapter 3 are very effective and easily implement-able on existing old types of cranes and can be sufficient to the requirements of the most of the job but still have few major draw backs as explained under:-

- a. Being open loop method, it has been assumed that no external disturbance exists. However, in actual the effects of wind (especially on large gantry cranes) and effect of unstable platform (like cranes on ship) can not be ignored.
- b. It has also been assumed that there is no oscillation at the start of movement which may not be possible at many places. These systems have no remedy under such circumstances.
- c. If by the mistake of operator or some system error oscillations are developed in the process of traversing, operator has no procedure or control to suppress them, being open loop systems.
- d. As mentioned in the Para 3.3.1, operator sends a pulse well in advance of the destination point so that the reduction in speed should take place in the same fashion as it was increased, demands operator expertise in estimating the distance when he

should send the pulse. This creates room for the mistake and damages.

- e. In comparison to a closed loop system, Demonstrated open loop crane takes little more time in shifting of load from one place to other. It consumes more time in increasing speed to maximum and similarly takes more time in deceleration to minimum. Operator has no control over changing these intervals of acceleration and decelerations.

In order to cater for these draw backs we also devised a closed loop method for oscillation by making use of newly emerging advance form of non linear control system technique i.e. Fuzzy Logic. We derived a nonlinear mathematical model of a rotary crane, which was used to run simulations under different operating conditions. The approach used two fuzzy logic controllers where each Fuzzy controller had two Fuzzy Inference Engines (FIEs) inside each, two for each degree of freedom. Computer simulations were run for the fuzzy controllers under different operating conditions i.e. Radial, Rotational, Compound and Damped cases. Simulation results showed that these controllers are able to damp any oscillations that might occur during the crane movement or generated even before movement but takes little longer time.

## **5.2 Recommendations**

As far as Open loop oscillation damping techniques, both the methods are very effective in controlling oscillation but have very less practical utilization especially in presence of external disturbance. Oscillation damping method utilizing fuzzy logic showed reasonable performance. But it took little more time in suppression of oscillation and also showed more overshoot of trolley in radial direction beyond the desired destination position so we can not say it the best controller. Keeping in view the results following is recommended for future investigation;-

- a. Further investigations is needed to consider the use of different membership functions in the fuzzy controller, such as Gaussian function and the modification of the rule structure of the rotational FIE

to account for the better coupling between the radial and rotational motions.

- b. As the error in the radial position turned out to be large, a change in the range of the radial error membership function may be considered to reduce the over shoot.
- c. Present fuzzy crane utilizes 142 rules which makes it computationally intensive and might be one of the reason of the over shoot in radial and rotational position especially in compound case. Attempt should be made to reduce the rule to make it computationally fast which will result in reduction of overshoot.
- d. For the practical demonstration of simulation results obtained in case of fuzzy crane, a two dimensional lab model should also be implemented.



### Matlab Code To Control Crane

```
clear all, clc;
for i=1:10; % Program written to demonstrate operation of crane for ten times.
    i=1;
    DIO1= digitalio('parallel','LPT1');    % To establish communication with p/port
                                           we define a variable
    addline(DIO1,0:7,'out');% Declares p/port as O/P port
    TS = 0;                                % min setting of voltage to give Trolley speed
                                           to produce acceleration of .02m/sec.
    putvalue(DIO1,TS);
    putvalue(DIO1.line(7),1);              % D6=0 cntris"OFF",D7=1 monitor ON/OFF of
                                           trolley motor
    Hoist_Length = input(' Enter Hoist Length (in Meters)= ');
    TimePeriod=(2*pi*sqrt(Hoist_Length/9.8))
    FD=2*TimePeriod/3    % FD is 1st Acceleration changing delay(in seconds)
    SD=TimePeriod/6      % SD is Subsequent Acceleration changing delay (in
                          seconds)
    DIO1= digitalio('parallel','LPT1');
    inreg = addline(DIO1,0:7,'in');        % Declares p/port as I/P port
    disp('MOVE TROLLY NOW')
    for j=1:1e30;                          % Loop to detect "TURN ON" of trolley motor
        j=1;
        ip= getvalue (inreg);
        if (ip(1,7)==0);                   % cond satisfied when trolley is moved and pin D7
                                           goes to '0' due to GND through ULN-2803
            break;
        end;
    end;
end;
tic                                         %Trolly move time is saved
```

```

disp('TROLLY HAS STARTED MOVING')
T1=clock; % used with "CVdelay"
for k=1:1e10; %CV infinite loop which end only when "D7=1"
    k=1;
    DIO1= digitalio('parallel','LPT1');
    addline(DIO1, 0:7, 'out');
    if (TS<15); % where "TS" is last supplied voltage.
        TS=TS+1;
        CVdelay; % for detail see CVdealy.m File given at the end of code
        putvalue(DIO1,TS); % Next Acceleration is applied
        putvalue(DIO1.line(7),1);
        T1=clock; % clock reset for calc next delay time
        FD=SD; % To keep subsequent delay as "TimePeriod/6"
    else
        putvalue(DIO1.line(1:8),[1 1 1 1 1 1 1 1]);
        % Above action Enables Cntr(D6=1),Latches decoder O/P& connects
        % D1~D5 with cntr ICs to read cntr value (D8=1).Monitoring of trolley
        % movement and stop pulse is still continued (D7=1).
        DIO1= digitalio('parallel','LPT1');
        inreg = addline(DIO1,0:7,'in');
        %To detect whether Reduce Acceleration pulse is given or not
        for L=1:1e10;
            L=1;
            ip=getvalue(inreg);
            if(ip(1,7)==1);
                break;
            end
        end
        end
        ip= ~(ip); %Inverted to get actual value as we used -ive Logic
        counter_reading= bin2dec('11111111111111')+ip(1)*2^14+ip(2)...
        *2^15+ip(3)*2^16+ip(4)*2^17+ip(5)*2^18; % 1st 14 bits are 1's

```

```

if (counter_reading>16383);
    totalrevolutions=counter_reading/500      % Optical Encoder gives
                                              500 pulses/rev.
    changeinlength=totalrevolutions*0.00028  %1 rev changes .028cms
    Hoist_Length=Hoist_Length-changeinlength;
end;
TimePeriod=(2*pi*sqrt(Hoist_Length/9.8))
SD=TimePeriod/6      % SD is Subsequent Acceleration changing delay
                    (in seconds)

for z=1:100;
    z=1;
    DIO1= digitalio('parallel','LPT1');
    addline(DIO1, 0:7, 'out');
    if (TS==0);          %To prevent from going TS to be"-ive"
        break
    end
    TS=TS-1;
    putvalue(DIO1,TS);   % lower Acceleration Voltage applied
    putvalue(DIO1.line(7),1);
    if(TS>=12)
        SD=.35;
    else
        SD=0.5;
    end
    T1=clock;
    CVdelay;
    T1=clock;
end %for loop
DIO1= digitalio('parallel','LPT1');
inreg = addline(DIO1, 0:7,'in');
for M=1:1e10;

```

```

        M=1;
        ip=getvalue(inreg);
        if (ip(1,7)==1);           %to detect Whether trolley is still moving or not
            break
        end
    end
    break;
end;
end
Trolley_Move_Time=toc;
disp('**TROLLY HAS STOPPED**---Trolley Move Time =')
disp(Trolley_Move_Time)
    Hoist_Length
end;
TS=0;
disp('Three loops completed')
DIO1= digitalio('parallel','LPT1');
addline(DIO1, 0:7, 'out');
putvalue(DIO1,TS);
CVdelay.m File
n=1;
for n= 1:1e9;
    T2=clock;
    T=etime(T2,T1);
    if (T>=FD);
        break;
    end;
end;
end;

```

# BIBLIOGRAPHY

- [1] Gantry crane, <http://www.femont.com/noord.jpg>.
- [2] Tower Cranes of America, <http://www.towercranes.com/Photo-Scans/30/30-13.jpg>.
- [3] Wilson J. Rugh “Linear System theory” .Prentice Hall, Upper Saddle River NJ.
- [4] K. Ogata. “Modern Control Engineering”. Prentice Hall, Upper Saddle River, NJ, 1997.
- [5] Ziyad N. Masoud ,“A Control System for the Reduction of Cargo Pendulations of Ship-Mounted Cranes”. Thesis submitted to the Faculty of the Virginia Polytechnic Institute and State University in partial fulfillment of the requirements for the degree of MS.
- [6] Myung Soo Moon, “Rule-Based Approaches for Controlling Oscillation Mode Dynamic systems”. Dissertation submitted to the Faculty of the Virginia Polytechnic Institute and State University for fulfillment of the requirements for the degree of Doctor of Philosophy.
- [7] “Method for inching a crane without load swing”  
<http://www.patentstorm.us/patents/6050429-description.html>
- [8] [http://en.wikipedia.org/wiki/Euler-Lagrange\\_equation](http://en.wikipedia.org/wiki/Euler-Lagrange_equation).
- [9] [http://en.wikipedia.org/wiki/Inverted\\_pendulum](http://en.wikipedia.org/wiki/Inverted_pendulum).
- [10] [http://en.wikipedia.org/wiki/Pendulum\\_\(mathematics\)](http://en.wikipedia.org/wiki/Pendulum_(mathematics)).
- [11] [http://en.wikipedia.org/wiki/Polar\\_moment\\_of\\_inertia](http://en.wikipedia.org/wiki/Polar_moment_of_inertia).
- [12] Math Works, Inc. MATLAB 7.0.0, R14 of May 2006.

- [13] Math Works, Inc. Version 2.0.1. SIMULINK, dynamic systems simulation for MATLAB 7.0.0, R14 of May 2006.
- [14] Math Works, Inc, "User guide Fuzzy logic toolbox 2", used with MATLAB 7.0.0, R14 of May 2006.
- [15] Li xing Wang, "A course in Fuzzy Systems and Control". Prentice Hall, Upper Saddle River, NJ.
- [16] Bart Kosko, "Fuzzy Engineering", Prentice Hall, Upper Saddle River, NJ.